SciPost Phys. Comm. Rep. 13 (2025)

Higgs production via vector-boson fusion at the LHC

Gaetano Barone[1★], Jiayi Chen[2†], Stephane Cooperstein[3‡], Nikita Dolganov[2∘],
Silvia Ferrario Ravasio[4§], Yacine Haddad[5¶], Stefan Höche[6∥], Barbara Jäger[7⋄],
Alexander Karlberg[4•], Alexander Mück[8⊙], Mathieu Pellen[9∨], Christian T. Preuss[10⊎],
Daniel Reichelt[4◁] Simon Reinhardt[7↻] and Marco Zaro[11✳]

1 Physics Department, Brown University, Providence RI, USA
2 Department of Physics, Simon Fraser University, Burnaby BC, Canada
3 University of California San Diego, 9500 Gilman Dr, La Jolla, CA 92093, USA
4 CERN, Theoretical Physics Department, 1211, Geneva 23, Switzerland
5 Northeastern University, Boston, MA, USA
6 Fermi National Accelerator Laboratory, Batavia, IL, 60510, USA
7 Institute for Theoretical Physics, University of Tübingen,
Auf der Morgenstelle 14, 72076 Tübingen, Germany
8 Institute for Theoretical Particle Physics and Cosmology,
RWTH Aachen University, 52056 Aachen, Germany
9 Albert-Ludwigs-Universität Freiburg, Physikalisches Institut,
Hermann-Herder-Str. 3, 79104 Freiburg, Germany
10 Institut für Theoretische Physik,
Georg-August-Universität Göttingen, 37077 Göttingen, Germany
11 TIFLab, Università degli Studi di Milano & INFN,
Sezione di Milano, Via Celoria 16, 20133 Milano, Italy

★ gaetano.barone@cern.ch , † jiayi.chen@cern.ch , ‡ stephane.b.cooperstein@cern.ch ,
∘ nikita_dolganov@sfu.ca , § silvia.ferrario.ravasio@cern.ch , ¶ yacine.haddad@cern.ch ,
∥ shoeche@fnal.gov , ⋄ jaeger@itp.uni-tuebingen.de , • alexander.karlberg@cern.ch ,
⊙ mueck@physik.rwth-aachen.de , ∨ mathieu.pellen@physik.uni-freiburg.de ,
⊎ christian.preuss@uni-goettingen.de , ◁ d.reichelt@cern.ch ,
↻ simon.reinhardt@uni-tuebingen.de , ✳ marco.zaro@mi.infn.it

*Part of the Report 5 Collection
published in the LHC Higgs Working Group Reports Series*

Abstract

In this article, we summarise the recent experimental measurements and theoretical
work on Higgs boson production via vector-boson fusion at the LHC. Along with this,
we provide state-of-the-art predictions at fixed order as well as with parton-shower cor-
rections within the Standard Model at 13.6 TeV. The results are presented in the form
of multi-differential distributions as well as in the Simplified Template Cross Section
bins. All materials and outputs of this study are available on public repositories. Finally,
following findings in the literature, recommendations are made to estimate theoretical
uncertainties related to parton-shower corrections.

1 Introduction

The unprecedented statistical accuracy and reduced systematics expected during the high-luminosity phase of the Large Hadron Collider (LHC) will make the study of the Higgs boson and the electroweak (EW) sector of the Standard Model an endeavor in precision physics. Higgs production via vector-boson fusion (VBF) is the mechanism with the second highest cross section after the gluon-fusion process and deserves particular attention due to its importance for the determination of the Higgs boson couplings. Its unique topology, characterised by the associated production of two jets with large invariant mass and large rapidity separation, makes it a relatively clean channel to study experimentally.

In order to study this mechanism in detail, it is crucial to have dedicated precise theoretical predictions within the Standard Model. In particular, given that VBF is typically measured in rather exclusive phase-space regions, inclusive predictions are not appropriate. To that end, we compile in the present study state-of-the-art predictions for the LHC at a centre-of-mass energy of 13.6 TeV at fixed order in common set-ups at the differential level.[1] It includes next-to-next-to-leading-order (NNLO) QCD corrections at the order $\mathcal{O}(\alpha_s^2\alpha^3)$, next-to-leading-order (NLO) EW corrections at the order $\mathcal{O}(\alpha^4)$, and irreducible contributions arising at orders $\mathcal{O}(\alpha_s^2\alpha^2)$, $\mathcal{O}(\alpha_s^3\alpha^2)$, and $\mathcal{O}(\alpha_s^4\alpha)$. As a by-product of our study, a comparison at leading-order (LO) and NLO QCD accuracy between calculations performed within and without the so-called VBF-approximation is also provided. In addition, several representative predictions are compared for predictions at NLO matched to parton showers (PS). This allows us to make recommendations for PS uncertainties for experimental analyses following existing findings in the literature [3–5]. It is worth emphasising that all the results (at fixed order and with parton showers) are obtained for multi-differential distributions as well as for Simplified Template Cross Section (STXS) bins [6].

Finally, we provide a review of theoretical progress and an explicit table with key references to be cited for specific types of calculations. In addition, recent experimental results by the ATLAS and CMS collaborations are also reviewed.

In order to ensure transparency we have made all the results and auxiliary data files publicly available at:

[https://gitlab.cern.ch/LHCHIGGSXS/LHCHXSWG1/VBFStudyYR5.](https://gitlab.cern.ch/LHCHIGGSXS/LHCHXSWG1/VBFStudyYR5)

In particular, input cards, possible customisations for the computer codes, RIVET [7] routines, and histograms are provided there. In addition, to allow experiments to perform benchmarks of event generators we have also stored there a subset of events used in the study.

The article is organised as follows: In Sec. 2, relevant theoretical work as well as recent experimental measurements are briefly reviewed. The computer programs used for the present study are described in Sec. 3. Section 4 summarises numerical input parameters, phase space definitions, as well as the observables considered in the subsequent numerical analyses. In Sec. 5, fixed-order results are discussed. In Sec. 6, several parton-shower predictions are compared and recommendations for the assessment of parton-shower uncertainties for VBF processes are given. Section 7 contains a summary of the study as well as some concluding remarks.

This work was carried out in the context of the LHC Higgs Working Group (LHCHWG) and in particular the VBF subgroup of the working group 1 (Higgs cross-section and branching ratios).[2]

---

[1]This is in contrast to typical predictions provided by the LHC Higgs Working Group (LHCHWG) which typically focus on inclusive predictions [1, 2].

[2]At https://twiki.cern.ch/twiki/bin/view/LHCPhysics/LHCHWG, a summary description of the various activities of the working group can be found.
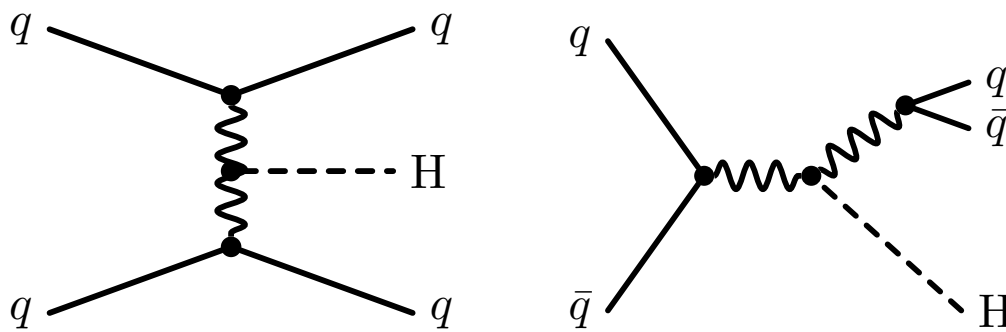
Figure 1: Examples of tree-level diagrams contributing to pp → Hjj: VBF (left) and VH (right) topologies.

2 Review of the state of the art

In this section, we review the theoretical and experimental status of VBF concentrating on the LHC. In particular, by providing Tables 2 and 3, we highlight the corresponding references.

2.1 Process definition

The EW production of an on-shell Higgs boson along with two jets that we are interested in can be described as the reaction

$$pp \to Hjj. \tag{1}$$

At leading order (LO) in perturbation theory, the process is defined at order $\mathcal{O}(\alpha^3)$. Interestingly, at this coupling order, the process contains both t- (and u-) and s-channel contributions. The former constitute the *VBF production* contributions. On the other hand, the latter is usually referred to as *V*H production or *Higgsstrahlung*. Here, *V* denotes either a W or Z boson that decays into a quark-antiquark pair. Sample Feynman diagrams of the two production mechanisms are displayed in Fig. 1.

An approximation, which is often used for VBF calculations, is to consider all t- and u-channel diagrams and square the contributions of these two topologies separately but do not take into account interferences between t- and u-channel diagrams. Also, s-channel contributions, as well as all interferences with them, are neglected. These types of interference contributions are typically small [8, 9]. The approximation is usually referred to as the *VBF approximation*, and this terminology will be used in the rest of the article. On the other hand, what we refer to as *full* computations enclose all possible contributions to the electroweak Hjj production process at a given order in perturbation theory, including interferences. We note that the predictions associated with both types of calculations are close to each other in phase space regions away from the s-channel resonances, *e.g.* when large invariant masses and rapidity differences between the two tagging jets are required. These are the phase space regions where VBF is measured experimentally.

2.2 Recent experimental measurements

Ten years after observing the Higgs boson, the current experimental accuracy reaches levels of $\approx 30\%$ on the total and inclusive cross-section in individual final states [10, 11]. Table 1 summarizes the latest sensitivity on the inclusive VBF signal of both ATLAS and CMS VBF results using the Run-2 dataset at $\sqrt{s} = 13$ TeV.

This unprecedented precision achieved with the proton-proton collision data recorded at the LHC Run 1 and Run 2 allowed for a more precise investigation of these production mech-

Table 1: Summary of experimental sensitivity on inclusive VBF signal at the LHC from ATLAS and CMS experiments.

	$\sigma/\sigma_{\mathrm{SM}}$	
Channel	CMS	ATLAS
$H \to \tau\tau$	0.86 ± 0.13 (stat) ± 0.05 (theo) ± 0.08 (exp) [12]	0.93 ± 0.12 (stat) ± 0.11 (syst) [13]
$H \to WW^*$	0.71 ± 0.26 [14]	0.93 ± 0.13 (stat) ± 0.16 (syst) [15]
$H \to \gamma\gamma$	1.04 ± 0.30 (stat) ± 0.06 (theo) ± 0.10 (exp) [16]	1.20 ± 0.18 (stat) ± 0.19 (syst) [17]
$H \to bb$	1.01 ± 0.50 [18]	0.99 ± 0.35 [19]
$H \to 4l$	0.48 ± 0.41 (stat) ± 0.12 (syst) [20]	1.21 ± 0.44 (stat) ± 0.06 (theo) ± 0.10 (exp) [21]

Table 2: Summary of most recent and most precise probes of VBF production modes at the LHC. The column on the left lists the references to Simplified Template Cross Sections and couplings results, while the column on the right the fiducial and differential cross section measurements.

Channel	ATLAS		CMS	
	STXS/coupling	Fiducial & differential	STXS/coupling	Fiducial & differential
Combination	[10, 22]	[23]	[11]	[24]
$H \to \gamma\gamma$	[17]	[25]	[16, 26]	[24, 26]
$H \to ZZ$	[21]	[27]	[20, 28, 29]	[24]
$H \to WW$	[15]	[30]	[14, 31]	[31]
$H \to b\bar{b}$	[19]		[18, 32, 33]	[32]
$H \to \tau\tau$	[13]	[13]	[12]	[24, 34]
$H \to \mu\mu$	[35]		[36]	
VBF$+\gamma$ $H \to b\bar{b}$	[37]			

anisms and VBF in particular. The STXS framework [6] provides a tool for combining the sensitivity of different Higgs boson decay channels for probing the couplings to fundamental particles at the production level. Both ATLAS and CMS have completed the experimental reach at Run-2, reaching the 10% level of precision individually [10, 11] on the combination from all available decay channels of Stage-0 STXS cross-section.

The further splitting of the production phase-space into m_{jj} and $p_{\mathrm{T}}^{\mathrm{H}}$ bins allows for setting stringent limits on new phenomena in a plethora of models and frameworks, such as Effective Field Theories, Supersymmetry, and generic coupling modifier frameworks. Beyond the channel-combined sensitivity, the LHC experiments have measured the VBF cross-section as a function of kinematic observables in single-channel decays. Fiducial measurements provide detector-independent cross-sections as a function of kinematic observables within a defined fiducial phase space. Organized by Higgs decay channels and measurement types - STXS or fiducial cross-section measurements, Table 2 summarises the references of the most recent results at Run-2 from the ATLAS and CMS experiments.

Projecting the total and inclusive cross-section measurements up to the first ab^{-1} of delivered luminosity at the LHC [38–40], their accuracy becomes limited by modeling uncertainties. The main limiting factor for the inclusive and total cross-sections remains the missing higher fixed-order calculations in both QCD and EW accuracies. However, the picture becomes more complex when going differentially and in the fiducial detector volume. The need for more segmented phase spaces stems from both a drive to measure the kinematic properties in the whole available phase space and from an experimental drive, where reconstruction techniques bring increased sensitivities in terms of background rejection when differentiating in terms of
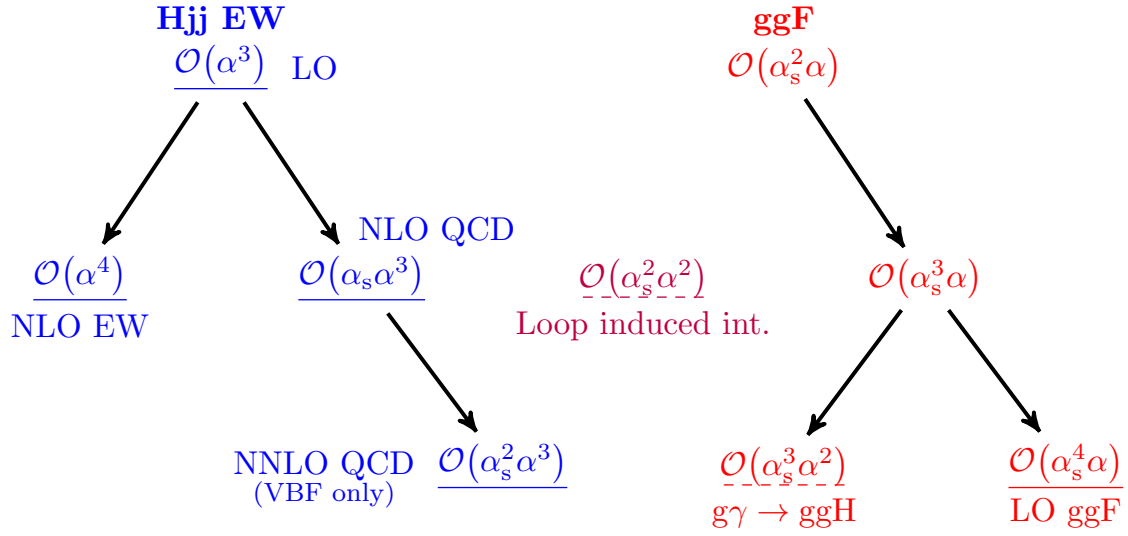
Figure 2: Graphical representation of higher-order contributions computed in the present work. See text for description.

the kinetic properties of the final-state particles. The limiting factor from the modeling uncertainties stems from parton-shower modeling (including also soft physics such a multi-parton interaction and hadronisation) and matching schemes. This is becoming a sizable contribution already for the first hundreds of fb^{-1} of delivered luminosity, as for example Ref. [15] gives relative VBF modeling uncertainties of 12%, which is large compared to the total uncertainty of 18% but also larger than what has been found in the present work or in Ref. [5].[3] Thus, looking ahead at the first ab^{-1} of proton-proton collisions at the LHC, it becomes evident that a coherent effort is needed to define a clear path for understanding and reducing these uncertainties.

2.3 Higher-order corrections

In this section, we discuss several processes and orders in perturbation theory that are contributing to the production of a Higgs boson in association with two jets. These contributions are summarised in Fig. 2. There, the blue contributions are the ones associated with the EW production of Hjj. The red ones are those associated with the gluon-gluon fusion process which is considered a background. The purple contribution cannot be unambiguously attributed to either of the two classes of process mentioned above. The (dashed-)underlined contributions are the ones that have been (partially) calculated for the present work.

2.3.1 QCD corrections

Factorisable QCD corrections for VBF At NLO, within the VBF approximation, QCD corrections to the upper and lower quark lines factorise. This inspired the so-called "structure-function approach" [41] which, by relying on the structure functions of deep-inelastic scattering (DIS), made it possible to compute NLO inclusive predictions for this process. Later on, the approach was extended to the fully differential case at NLO QCD [42,43] and implemented in the parton-level Monte-Carlo generators VBFNLO [44–46] and MCFM, and to NNLO QCD [47,48], where gluon exchange between the two quark lines is non-zero, but still color-suppressed. Finally, NNNLO QCD corrections were also computed for the inclusive case [49].

---

[3]We note that the uncertainty estimate of Ref. [15] also includes hadronisation effects which is not the case for the present work or Ref. [5].
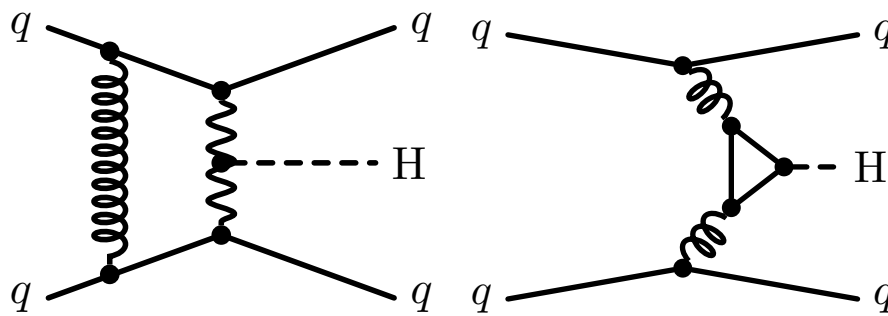
Figure 3: Examples of non-factorisable corrections (left) and loop-induced contributions (right).

Nowadays, two calculations are available for the differential computation of cross section at NNLO QCD accuracy [50, 51] in the VBF approximation.

Note that in Ref. [52], NNLO QCD corrections to both production of a Higgs boson via VBF and its decay into a bottom-antibottom quark pair were considered for the first time. The corrections to the full process with Higgs decay products are larger than in the inclusive case with a stable Higgs due to the constrained phase space on the decay products. In Ref. [53], the description of the decay part was improved from NNLO QCD to NNLO QCD+parton shower accuracy. The inclusion of all-orders resummation provided by the parton shower in the decay reduces the fiducial cross section by about 10%.

Non-factorisable QCD corrections for VBF   At NNLO-QCD, the factorised picture discussed above breaks down due to gluon exchange between the two quark lines, cf. Fig. 3 (left). The one-loop diagram shown there enters already at NLO-QCD, but at this order it enters only through the interference with the Born diagram, and since the exchanged EW bosons do not carry colour this contribution vanishes due to colour conservation. At NNLO-QCD the squared diagram and also the interference between the two-loop diagram and the Born diagram enter. Formally, they are colour-suppressed since the exchanged gluons have to form a colour-singlet, but at the precision at which other contributions to VBF are currently known, they cannot be neglected.

The full computation of the non-factorisable corrections at NNLO-QCD is not within the scope of current technology, but significant progress has been made in computing them in the so-called eikonal approximation. In Ref. [54] the leading eikonal term was for the first time computed, and the corrections to VBF within typical cuts were found to range between a few per mille and a per cent. More differential studies were carried out in Ref. [55] where the calculation was also extended to di-Higgs VBF production. Since then the original work has been complemented with sub-leading eikonal effects and full real-emission matrix elements [56–58]. In this study we only consider the leading eikonal contributions.

QCD corrections to the full EW pp → Hjj production   As previously discussed, in the VBF approximation, one disregards s-channel contributions stemming from associated VH production where the vector boson V decays hadronically, as well as interferences between t- and u-channel contributions. This approximation is accurate in typical VBF fiducial regions while it is not very accurate in inclusive phase space regions [48, 59, 60]. The full calculations at NLO QCD accuracy are available for up to H + 3j [60, 61]. The limiting factor for computing the complete VBF process at NNLO QCD is the availability of the two-loop virtual corrections.

2.3.2 EW corrections

The virtual EW corrections consist of all possible one-loop insertions of EW particles to the Born process. On the other hand, for the real emission corrections, only photon radiation is taken into account. Contributions due to the emission of massive weak bosons are not included, as they are not needed to cancel infrared divergences in the virtual corrections, and can be removed from experimental analyses via appropriate vetoes.

Electroweak corrections have initially been computed for the full EW pp → Hjj production in Ref. [59], and for the VBF approximation in Ref. [62]. Typically, for current hadron colliders, the corrections are at the level of a few per cent for fiducial cross sections. On the other hand, for differential distributions, they can become large in parts of the phase space. Usually in the high-energy limit, they become negatively large because of Sudakov logarithms while below resonances, they are positive due to real photonic emissions.

To obtain fixed-order predictions at NLO EW accuracy, dedicated codes like HAWK [63] or multi-purpose codes like MADGRAPH5_AMC@NLO [64] or SHERPA 3 [65] are publicly available. Electroweak corrections to both the VBF-approximated and the full process can be obtained.

2.3.3 Irreducible contributions

The NLO QCD corrections to the hadronic EW process pp → Hjj are of the order $\mathcal{O}(\alpha_s \alpha^3)$ while the NNLO QCD corrections are order $\mathcal{O}(\alpha_s^2 \alpha^3)$. For the process at hand, loop-induced amplitudes of order $\mathcal{O}(\alpha_s^2 \sqrt{\alpha})$ also exist, as depicted on the right-hand side of Fig. 3. They can be interfered with the EW production to provide $\mathcal{O}(\alpha_s^2 \alpha^2)$ contributions or squared to raise $\mathcal{O}(\alpha_s^4 \alpha)$ contributions. These types of corrections are separately infrared finite and are typically rather suppressed.

The corrections of order $\mathcal{O}(\alpha_s^2 \alpha^2)$ have been computed first in Ref. [66] in the infinite top-mass limit for the t and u channels. In Ref. [67,68], NLO QCD corrections to the interferences i.e. contributions of order $\mathcal{O}(\alpha_s^3 \alpha^2)$ have been computed and found to be negligible for experimental measurements. The contributions presented here therefore constitute an update with respect to Ref. [66] by providing full top-mass dependence as well as all channels (including s-channel contributions).

The contributions of order $\mathcal{O}(\alpha_s^4 \alpha)$ are formally part of the NNLO QCD corrections to the production of a Higgs boson via gluon-gluon fusion. In Refs. [70, 71], state-of-the-art corrections to the order $\mathcal{O}(\alpha_s^4 \alpha)$ have been presented, unfortunately in phase-space regions not typical for VBF measurements. In the present work, we provide the $\mathcal{O}(\alpha_s^4 \alpha)$ contribution for the quark-induced channels with full top-mass dependence which is a truly irreducible IR-finite contribution. In addition, we also provide the complete set of contributions that include external gluons. We refer to the latter as *LO ggF* as they correspond to the LO contribution to the gluon-gluon fusion process when requiring two identified jets.

In Ref. [69], the gluon-gluon induced contribution for Higgs production via vector-boson fusion in a loop-induced process and contributing at $\mathcal{O}(\alpha_s^2 \alpha^3)$ was computed. It is formally part of the NNLO QCD correction to VBF with a gluon-gluon initial state instead of the quark-quark one. Due to its smallness, this contribution has not been reproduced here.

Finally, for completeness the loop-induced contribution gγ → ggH appearing at order $\alpha^2 \alpha_s^3$ has also been computed. Due to its dependence on the photon PDF and the relevant coupling factors, it is strongly suppressed, justifying why it has never been reported publicly before.

2.3.4 Parton showers

Parton showers are the key component of general purpose Monte Carlo (GPMC) event generators, such as HERWIG 7 [72,73], PYTHIA 8 [74,75], and SHERPA 3 [65,76–78], as they enable a

full-fledged description of collider events by including the dominant logarithmically-enhanced QCD corrections at all orders.

In order to improve the description of inclusive quantities, such as total cross sections, and the modelling of hard QCD radiation, parton showers are routinely combined with fixed-order calculations, via a careful matching procedure that prevents the double counting of contributions present both in the shower and in the fixed-order calculation. Higgs production via VBF has been available at NLO+PS accuracy for more than a decade (see, *e.g.* Refs. [79,80]). Comparative studies assessing the uncertainty of such generators from parton shower and matching variations can be found, *e.g.* in Refs. [3–5]. In general, considering these variations leads to a $10 − 15\%$ uncertainty for inclusive distributions. An important observation is the particular sensitivity of this process to QCD colour-coherence effects, which highly suppress the presence of radiation at central rapidities. The use of parton showers which violate this property can lead to fictitiously large uncertainties [3, 4, 81], and must be avoided. Beyond NLO matching, it is also possible to combine calculations with several jet multiplicities (*e.g.* 2 and 3) up to NLO via multi-jet merging [4, 82].

Another direction of improvements involves the inclusion of s-channel contributions and related interferences [60, 83] alongside the ones defining the VBF topology. Nowadays all the NLO+PS event generators that support VBF production can also handle the full pp → Hjj EW production mode [5]. The inclusion of NLO EW corrections is also a currently ongoing endeavour. So far they have been implemented only in Ref. [83], albeit they are not (yet) combined with NLO QCD corrections.

Recent years have seen also a renewed interest in the formal accuracy of parton-shower algorithms. In particular, the first shower with general next-to-leading logarithmic (NLL) accuracy for VBF (in the factorised approach) was presented in Ref. [84]. Accurately matching NLL-accurate showers to NLO QCD calculations for complex processes such as VBF is still work in progress, and for this reason we refrain from including higher-logarithmic parton-shower algorithms in our study.

The general purpose event generators and the NLO event generators that we consider in this study are listed in Secs. 3.2 and 3.3, respectively. In this study, we focus only on the perturbative components of GPMC simulations, although PS simulations are embedded in a framework to consistently incorporate soft-physics effects, such as hadronisation and multi-parton interactions. A comprehensive study of these soft-physics effects in the context of the HERWIG 7 event generator can be found *e.g.* in Ref. [85], while a first estimate in the context of the PYTHIA 8 event generator was performed in Ref. [4].

3 Computer programs

In this section we describe the computer programs used in our study.

3.1 Fixed-order programs

3.1.1 HAWK

HAWK [63] provides fully differential parton-level predictions for Higgs boson production in Higgs-strahlung [95] and vector-boson fusion [59, 62] including the complete NLO QCD and EW corrections. For the VBF channel, t-channel, u-channel, and s-channel contributions and the corresponding interference contributions are all available. Photon-induced channels as part of the EW NLO corrections are also included. Interference contributions between VBF diagrams and gluon-fusion diagrams, as discussed in Section 2.3.2, are also available. Partonic channels with bottom quarks in the initial or final state are only supported

Table 3: Summary of references for theory work in VBF at the LHC.

Code	References
Fixed order	
VBF approximation and higher multiplicity	[42, 43, 48, 59–61]
NLO EW	[59, 62, 86]
NNLO QCD (in VBF approx.)	[50–53, 87]
N3LO QCD (inclusive)	[49]
Non-factorisable corrections	[54–58, 88]
Irreducible background	[66, 67, 69]
Background process	[70, 71, 89–93]
Boosted Higgs	[5, 94]
Parton showers and event generators	
NLO matching in VBF	[79, 80, 83]
Multi-jet merging in VBF	[4, 82]
NLO+PS uncertainties in VBF	[3–5]
Soft-physics effects in VBF	[4, 85]
NLL showers in VBF	[84]

at leading order. External fermion masses are neglected. Anomalous Higgs boson–vector-boson couplings are supported starting from version 2.0. The code is publicly available from https://hawk.hepforge.org.

In the present work, HAWK has been used to validate the full calculations performed by MOCANLO+RECOLA at LO, NLO QCD, and NLO EW accuracy as well as the contribution of order $\mathcal{O}(\alpha_s^2 \alpha^2)$. In addition, HAWK has been used to check the LO and NLO QCD prediction of PROVBF in the VBF approximation. Beyond LO, the checks have been performed upon omitting the bottom-quark contributions.

3.1.2 PROVBF

PROVBF [49, 50, 96, 97] is a tool which computes NNLO- and N3LO-QCD corrections to both single and double Higgs production through VBF in the factorised approximation. At NNLO it is fully differential in the kinematics of the jets. It uses the projection-to-Born method to achieve this using parametrised NNLO structure functions [98, 99] as implemented in HOP-PET [100] and a fully differential VBF H+3jet NLO calculation from the POWHEG-BOX [79, 101, 102]. The leading eikonal non-factorisable corrections, first computed in Ref. [54], are also available [55]. The code is publicly available from https://github.com/alexanderkarlberg/proVBFH.

In the present work, PROVBF has been used to provide the NNLO QCD and the leading eikonal non-factorisable corrections in the VBF approximation.

3.1.3 MOCANLO+RECOLA

The combination MOCANLO+RECOLA relies on the flexible Monte Carlo program MOCANLO and the matrix-element generator RECOLA [103, 104]. With this at hand, any processes in the Standard Model can be computed at full NLO accuracy *i.e.* with QCD, EW, or mixed QCD-EW corrections.

For the one-loop corrections, RECOLA relies on the COLLIER library [105, 106] to numerically evaluate the one-loop scalar and tensor integrals. On the other hand, infrared divergences are handled with the Catani–Seymour dipole formalism for all singularities of QCD and QED type [107, 108]. Additionally, there is the option to use the FKS subtraction scheme [109] for final-state QCD corrections [110]. The program has been successfully used to compute NLO QCD and NLO EW corrections to double-Higgs production via VBF [111] as well as several VBS processes [112–117].

In the present work, full predictions, *i.e.* including all topologies and their interferences at LO, NLO QCD, and NLO EW accuracy have been obtained from MOCANLO+RECOLA. In addition, the irreducible contributions of orders $\mathcal{O}(\alpha_s^2\alpha^2)$, $\mathcal{O}(\alpha_s^3\alpha^2)$, and $\mathcal{O}(\alpha_s^4\alpha)$ have also been obtained from MOCANLO+RECOLA.

3.2 General purpose event generators

3.2.1 HERWIG 7

HERWIG 7 [72, 73, 118] is a general-purpose event generator, known for its unique angular-ordered parton shower [119], which generalises the algorithm implemented in its predecessor HERWIG [120], and for its hadronisation cluster model [121]. HERWIG 7 also includes a transverse-momentum ordered dipole shower [122].

HERWIG 7 is the event generator that allows for the largest variety of matching methods. First of all, it supports the matching with events generated with external NLO generators via the standard Les Houches interface [123]. Secondly, it implements a dedicated `Matchbox` [124] module, which enables to combine NLO QCD calculations with both the angular-ordered and dipole showers using the POWHEG [125] or MC@NLO [126] method.[4] In the case of the dipole shower, `Matchbox` also offers the possibility to perform NLO multi-jet merging via the unitarised merging scheme [128]. A dedicated study of multi-jet merging for VBF and the full EW Hjj process can be found in Ref. [82].

In the context of this study, we will consider the following NLO+PS predictions:

- angular-orderd parton showering on top of NLO events generated with POWHEG-BOX (see Sec. 3.3.2) or MADGRAPH5_AMC@NLO (see Sec. 3.3.1).

- internal NLO matching in the MC@NLO scheme with both the angular-ordered and the dipole parton shower.

For the latter, we use HERWIG7.3.0, and dedicated matrix element providers. In particular, for this study we employ VBFNLO and HJETS++ for the simulation of VBF and the full EW Hjj production.

- VBFNLO [44–46, 129] is a flexible parton-level Monte-Carlo program for processes with EW bosons. Besides the Standard Model, also a variety of new-physics models including anomalous couplings of the Higgs and gauge bosons are accounted for. For the VBF-H process, it can compute NLO QCD and EW corrections. The WH production process and several irreducible backgrounds to VBF are also available.

- HJETS++ [60] is a dedicated code for the calculation of the EW production of a Higgs boson accompanied by up to 3 jets at NLO QCD, including both VBF and Higgs-Strahlung contributions, as well as their interference.

---

[4]For processes such as Drell-Yan, also the KRKNLO method is available [127].

3.2.2 PYTHIA 8

The PYTHIA 8 package [74, 75] is a multi-purpose particle-level event generator, with a historically strong focus on the modelling of soft physics. A core component of PYTHIA 8 is its hallmark string fragmentation model [130, 131], which models the non-perturbative transition from coloured partons to colourless hadrons. The default PYTHIA 8 shower, which we refer to as the "simple shower", is a p_T-ordered parton shower based on DGLAP kernels [132]. Rooted in the p_T-ordered DGLAP evolution, this default option does not, however, correctly account for soft coherence effects, which are particularly important in processes such as VBF [3, 4, 81]. Its use in such processes is therefore discouraged. A dipole-recoil option is, however, available for the simple shower. This replaces the independent evolution of the initial- and final-state legs in initial-final colour dipoles with a coherent, antenna-like evolution [133]. In its present 8.3 series, PYTHIA 8 offers the VINCIA [134] and DIRE [135] parton-shower algorithms as alternatives to its default shower implementation. In either case, multi-parton interactions are simulated in a fully-interleaved sequence with the shower [132].

A wide range of multi-jet merging schemes is available with PYTHIA 8. Internally, merging is performed in the CKKW-L scheme [136] at leading order and in the UNLOPS scheme [137] at next-to-leading order. While NLO matching schemes are not implemented internally, PYTHIA 8 can be interfaced to either MADGRAPH5_AMC@NLO in the MC@NLO [126] scheme or POWHEG-BOX in the POWHEG [125] scheme. In the case of the former, the matching is tied to the simple shower with a (non-default) global recoil scheme for final-state branchings to match the MC@NLO counter terms implemented in MADGRAPH5_AMC@NLO. In the case of the latter, dedicated `PowhegHooks` are available for all three shower models, to account for the mismatch between the shower ordering variable and the POWHEG evolution scale [138]. A practically important setting of the `PowhegHooks` is the `POWHEG:pThard` mode, which controls the selection of the "hard" scale of the POWHEG event above which further radiation is vetoed. While in principle equivalent up to the formal accuracy of the matching scheme, large parametrical uncertainties of different choices have been observed for processes which contain jets at the Born level [4, 139, 140]. The default choice is `POWHEG:pThard = 0`, which corresponds to using the scale provided in the event file (`scalup`), as the hard scale for the shower evolution. Each time an emission is produced, its transverse momentum p_T according to the POWHEG definition is computed and the emission is vetoed if the shower p_T is larger than `scalup`. Another suitable choice is to recalculate the POWHEG scale as the minimal POWHEG p_T across the event [4, 139, 141], corresponding to the setting `POWHEG:pThard = 2`.

In the context of this study, the simple shower with dipole recoil and the VINCIA antenna shower are applied. NLO matching is performed in the POWHEG scheme, using event input from POWHEG-BOX. The influence of the evolution-variable mismatch between POWHEG-BOX and the parton showers is mitigated by the use of vetoed showers via `PowhegHooks`.

3.2.3 SHERPA 3

SHERPA 3 [65, 76–78][5] is a general-purpose particle-level event generator. Its development began during the late days of the LEP experiments and primarily targeted the LHC. SHERPA 3 includes the two automated matrix-element generators AMEGIC [142] and COMIX [143], which are used in combination [123, 144] with various one-loop providers to compute the fixed-order input for NLO matching and multi-jet merging. Matching is performed using the S-MC@NLO method [145] and merging is achieved at leading order in the CKKW-L method [146], and at next-to-leading order in the MEPS@NLO method [147]. In this study, we consider both the VBF-induced and the full EW Hjj production mode. For this study, SHERPA 3 implements

---

[5]The predictions here are based on the Sherpa 3.0 release, including bugfixes that will be made available with version 3.0.2, and have been validated to give identical results to the patched SHERPA version used in [5].

the one-loop virtual corrections to VBF in the structure function approximation [5], i.e. including vertex corrections for the color connected quark dipoles only, and interfaces to OPEN-LOOPS [148,149] for the one-loop virtual corrections to the full EW pp → Hjj process. For the predictions shown in this study we employ both SHERPA 3's default parton shower [150], sometimes referred to as the CS shower, and the DIRE parton shower [135]. Infrared subtraction at fixed order QCD is carried out using the Catani-Seymour dipole factorization method [107], in the case of DIRE adapted to the splitting kernels in this parton shower. The subtraction is implemented in both AMEGIC [151] and Comix.

3.3 NLO event generators

3.3.1 MADGRAPH5_AMC@NLO

The metacode MADGRAPH5_AMC@NLO [64,152] makes it possible to simulate arbitrary processes including NLO QCD and EW corrections, and to perform the matching to PS with the MC@NLO method [126] in the former case. The computation of NLO corrections relies on the FKS subtraction scheme [109,153–155] for what concerns the local subtraction of IR divergences, and on MADLOOP [156], which in turns employs several one-loop reduction techniques [148,157–161] implemented in third-party tools (CUTTOOLS [162], IREGI [163], NINJA [164, 165], COLLIER [105, 106]), which are either shipped with the main code, or can be installed at the user's request. The simulation of VBF-H production within MADGRAPH5_AMC@NLO has been documented in Refs. [3, 80]. As explained in the latter work, the simulation of Higgs production via VBF at NLO-QCD accuracy can be performed issuing the commands:

```
import model loop_qcd_qed_sm_Gmu
generate p p > h j j $$ w+ w- z [QCD]
output
```

The syntax `$$ w+ w- z` vetoes those diagrams with W or Z bosons in the *s*-channel. Furthermore, the default behaviour of MADGRAPH5_AMC@NLO includes only those loops made entirely up of QCD-interacting particles,[6] whereas tree-level interferences are always considered. In this study we also consider the full EW Hjj production mode, that can be simulated omitting `$$ w+ w- z`.

Finally, let us discuss the matching to PS. In principle both PYTHIA 8 [75,166] and HERWIG 7 [72, 73, 118] parton showers can be employed. However, as already discussed in Sec. 3.2.2, it has been shown that the global-recoil scheme employed in PYTHIA 8 for which the MC@NLO counterterm have been derived is unfit for VBF while other schemes, such as the dipole recoil scheme [133], should be employed. In the lack of MC@NLO counterterms compatible with such a scheme, we only employ the HERWIG7 (specifically, version 7.2.1 [118]) angular-ordered shower [119] for matched predictions.

3.3.2 POWHEG-BOX

The POWHEG-BOX [101] is a general framework for the matching of NLO calculations with parton-shower (PS) programs according to the POWHEG prescription [125,167]. Dedicated implementations have been provided for the VBF-induced Hjj process at NLO-QCD matched to PS in Ref. [79], and for the Hjjj process in Ref. [102]. In Ref. [83] the full EW Hjj production process, including both VBF and Higgsstrahlung topologies, has been accounted for with amplitudes provided by RECOLA 2 [168] in the framework of the POWHEG-BOX-RES [169], a

---

[6]If the EW-capable v3 [64] is employed, such a limitation can be lifted. However, because of the tininess of these contributions, we opt for not including them.

version of the POWHEG-BOX specifically designed to handle processes with a complicated resonance structure or competing topologies. This latter implementation of the full EW Hjj process allows for a matching of NLO-QCD and NLO-EW corrections to a PS generator. In this study we consider the NLO+PS generator for the VBF-induced contribution [79], as well as the one for the full EW Hjj production [83]. Events are showered with the HERWIG 7 angular-ordered parton shower (v 7.2.3 [118]) and with PYTHIA 8 (v 8.315) [75].

3.4 Other tools not used in this study

For completeness, we here provide a short description of computer programs which are relevant for VBF studies but which have not been used for the present study.

- HEJ is a Monte Carlo event generator for hadronic scattering processes at high energies [92, 170–174]. It provides all-order summation of the perturbative terms dominating the production of well-separated multiple jets at hadron colliders. These processes involve pure multijet production, gluon-fusion production of a Higgs boson with jets, the production of a W boson with jets, two same-sign W bosons with jets or jets with a charged lepton-antilepton pair, via a virtual Z boson and/or photon. Several studies have been particularly focusing on Higgs production in association with two jets as defined in Sec. 2.3.3 [71, 91–93, 170, 171]. The code is publicly available from https://hej.hepforge.org.

- WHIZARD is an event generator, able to compute NLO EW corrections as well as NLO QCD corrections matched to parton shower for arbitrary processes [175,176]. The code is publicly available from https://whizard.hepforge.org.

4 Computational set-up

4.1 Input parameters

The present input parameters are the ones recommended by the Higgs cross section working group for run-III predictions.[7] The results obtained in the present work are for the LHC running at a centre-of-mass energy of $\sqrt{s} = 13.6\,\text{TeV}$. We use the PDF4LHC21_40 parton distribution function (PDF) set [177,178] for quarks and gluons via the LHAPDF interface [179]. This PDF set employs $\alpha_\text{s}(M_Z^2) = 0.118$ for the strong coupling constant. For photon-induced contributions, the set LUXqed17_plus_PDF4LHC15_nnlo_100, which relies on the method of Ref. [180] for the extraction of the photon distribution, is used.

The following masses and widths are used:

$$
\begin{aligned}
2m_\text{t} &= 172.5\,\text{GeV}\,, & m_\text{b} &= 0\,\text{GeV}\,, \\
M_Z &= 91.1876\,\text{GeV}\,, & \Gamma_Z &= 2.4952\,\text{GeV}\,, \\
M_W &= 80.379\,\text{GeV}\,, & \Gamma_W &= 2.085\,\text{GeV}\,, \\
M_H &= 125.0\,\text{GeV}\,, & \Gamma_H &= 0\,\text{GeV}\,.
\end{aligned}
\tag{2}
$$

The EW coupling is fixed in the G_μ scheme [181, 182] upon using

$$
\alpha = \frac{\sqrt{2}}{\pi} G_\mu M_W^2 \left(1 - \frac{M_W^2}{M_Z^2}\right)\,, \qquad \text{and} \quad G_\mu = 1.16638 \times 10^{-5}\,\text{GeV}^{-2}\,.
\tag{3}
$$

---

[7]These can be found at https://twiki.cern.ch/twiki/bin/view/LHCPhysics/LHCHWG136TeVxsec.

The numerical value thus obtained reads $\alpha = 0.75652103079904 \times 10^{-2}$. The same convention (with different input values) has been used in several comparatives studies, *e.g.* Refs. [81,183].

Finally, following Ref. [50], for the renormalisation and factorisation scales, μ_R and μ_F, the default central values μ_0 used in our calculation are obtained from

$$\mu_0^2 = \frac{m_H}{2} \sqrt{\frac{m_H^2}{4} + p_{T,H}^2}, \tag{4}$$

where m_H and $p_{T,H}$ are the mass and the transverse momentum of the Higgs boson, respectively. In the following, scale uncertainties are estimated by a seven-point variation of μ_R and μ_F.[8]

4.2 Phase-space definitions

For this study, three different phase space volumes were investigated: the STXS one [6],[9] and two fiducial ones. It is worth pointing out that the fiducial volumes have been designed in collaboration with experimentalists of both the ATLAS and CMS collaborations. These fiducial regions could be used for the combination of ATLAS and CMS results as well as for future comparisons of theoretical predictions with experimental measurements.

STXS set-up   This setup follows the definition provided in Ref. [6]: Two jets reconstructed with the anti-k_T algorithm [185] with $R = 0.4$ are required with transverse momenta

$$p_{T,j} > 30\,\text{GeV}, \tag{6}$$

and no rapidity constraints. In addition, the Higgs boson should be central,

$$|\eta_H| < 2.5. \tag{7}$$

Fiducial setup (a)   The fiducial definitions are less inclusive. For the first one, again two anti-k_T jets with $R = 0.4$ are required, this time with

$$p_{T,j} > 30\,\text{GeV}, \quad \text{and} \quad |\eta_j| < 4.7. \tag{8}$$

In addition, the two hardest jets in the rapidity range $|\eta_j| < 4.7$ should fulfill

$$m_{jj} > 300\,\text{GeV}, \quad \text{and} \quad |\Delta y_{jj}| > 2. \tag{9}$$

There are no event selection requirements applied to the Higgs boson, in contrast to the STXS set-up.

---

[8]Notice that this choice of μ_0 differs from the one adopted in Ref. [5], *i.e.* $\mu_0 = H_T^2/4$, with

$$H_T = \sqrt{m_H^2 + p_{T,H}^2} + \sum_{i \in \text{partons}} p_{T,i}. \tag{5}$$

We have, however, verified for both NLO QCD and NLO QCD+PS predictions that the two choices for the central renormalisation, factorisation, and shower starting scale are compatible within the usual seven-point scale variations. We discuss the variation of these scales in the context of NLO+PS in Sec. 6.

[9]It is worth mentioning that the 1.2 stage of the STXS is identical to the 1.1 stage [184].

Fiducial setup (b) The definition of the second fiducial volume is similar to the first one, apart from the requirement on the jets' minimum transverse momenta, which is changed from Eq. (8) to

$$p_{\mathrm{T,j}} > 20\,\mathrm{GeV}, \quad \text{and} \quad |\eta_{\mathrm{j}}| < 4.7\,. \tag{10}$$

The cuts of Eq. (9) on the two hardest jets are retained.

The **fiducial (a)** and **fiducial (b)** setups are rather similar, but are nonetheless considered here as the ATLAS and CMS collaborations sometimes use different transverse-momentum requirements in their measurements.

In the following, the two hardest jets fulfilling the requirements of Eq. (6) for the STXS setup, of Eq. (8) for the **fiducial (a)** phase space, and of Eq. (10) for the **fiducial (b)** phase space, will sometimes be referred to as the *tagging jets*. When not stated explicitly, the two jets appearing in differential distribution are always the tagging jets.

4.3 Observables

In this work and in the repository associated to it, several characteristic LHC observables are considered. Typical one-dimensional distributions are provided, and in addition specific multi-dimensional bins are presented.

STXS set-up In the STXS set-up, the usual multi-dimensional bins (provided in Ref. [6]) in the invariant mass of the two hardest jets, the transverse momentum of the Higgs boson, and the transverse momentum of the combined Higgs boson with two jets are given. All these bins are further divided into $\Delta\phi_{\mathrm{jj}}$ bins for $[0;\pi/2]$ and $[\pi/2;\pi]$ making the distribution effectively four-dimensional. Here, the variable $\Delta\phi_{\mathrm{jj}}$ is defined as the absolute value of the azimuthal angle between the two tagged jets. In the SM, the distribution is symmetric about $\Delta\phi_{\mathrm{jj}} = 0$. In Sec. 5.1, this distribution will only be shown while integrating over the transverse momentum of the combined Higgs boson with the two jets in order to ease readability.

Fiducial setups (a) and (b) For these fiducial set-ups, several two-dimensional distributions are provided: $m_{\mathrm{jj}} \times p_{\mathrm{T,H}}$, $m_{\mathrm{jj}} \times \Delta\phi_{\mathrm{jj}}$, $m_{\mathrm{jj}} \times \Delta y_{\mathrm{jj}}$, and $p_{\mathrm{T,H}} \times \Delta y_{\mathrm{jj}}$. The ranges and the exact binning are provided in the repository. The ranges are chosen so that these bins can be individually measured at the end of the high-luminosity LHC in typical experimental analyses. These are discussed in Sec. 5.2.

5 Fixed-order predictions

In this section, fixed-order results are discussed for the fiducial volumes introduced above and the STXS setup which is particularly inclusive. Various aspects are discussed, ranging from the VBF approximation, QCD and EW corrections to irreducible contributions.

At fixed order, we define the best prediction as

$$\sigma_{\mathrm{best}} = \sigma_{\mathrm{NLO\,QCD}}^{\mathrm{Full}} \times \left(1 + \delta_{\mathrm{NNLO\,QCD}}^{\mathrm{VBF}} + \delta_{\mathrm{NNLO\,QCD}}^{\mathrm{NF\,VBF}}\right) \times \left(1 + \delta_{\mathrm{NLO\,EW,\,no\,}\gamma}^{\mathrm{Full}}\right) + \Delta_{\gamma}^{\mathrm{Full}}, \tag{11}$$

where $\sigma_{\mathrm{NLO\,QCD}}^{\mathrm{Full}}$ designates the NLO QCD cross section in the full calculation *i.e.* also including the VH contributions and its interference with VBF. The various relative corrections are defined as

$$\delta_k^i = \frac{\Delta_k^i}{\sigma_{\mathrm{LO}}^i}\,, \tag{12}$$

where the Δ_k^i are the corrections of type k expressed in units of the cross section. The index i indicates whether a specific correction refers to the full calculation, the VBF-approximated one or the non-factorisable corrections in the VBF approximation. Note that the photon-induced corrections are not included in the relative EW corrections but singled out and denoted by $\Delta_\gamma^{\text{Full}}$. It is worth pointing out that this combination of the various corrections is a simple extension of what has been used in the past for inclusive predictions within the HXSWG [1,2].

This definition of the best prediction in Eq. (11) is trivially extended from the cross section to differential distributions as well. Note that in parts of the phase space where the VBF approximation is not reliable, only NLO QCD accuracy is achieved with this approach. For example, for the STXS binning, for bins with $m_{\text{jj}} < 350\,\text{GeV}$, the NNLO QCD corrections in the VBF approximation are set to zero in Eq. (11) reflecting the fact that NNLO QCD corrections are not known in this part of the phase space. An improvement of this approximation would require including NNLO QCD contributions for VH production where the W and Z bosons decay into jets.

As mentioned above, for the results presented in the following, the LO, NLO QCD, NNLO QCD and non-factorisable corrections in the VBF approximation have been obtained from PROVBF. All the other full contributions/corrections, MOCANLO+RECOLA has been used to provide the results. For all LO and NLO corrections, HAWK has been used to successfully validate the results of both PROVBF and MOCANLO+RECOLA.

5.1 STXS setup

First, we consider the invariant-mass distribution of the tagging jets within the STXS setup of Eqs. (6)–(7). In Fig. 4, the uppermost panel shows the LO result within the VBF approximation as well as the best prediction obtained using the prescription of Eq. (11). The second panel illustrates the ratio of the predictions at LO and NNLO within the VBF approximation, and the NF QCD corrections to the VBF NLO QCD result. The third panel of Fig. 4 displays the EW corrections as well as the photon-induced contributions for the full calculation. The fourth panel shows the size of the non-VBF contributions at both LO and NLO QCD. Finally, the two lowest panels show the size of three types of contributions: loop-induced interference, loop-induced squared, and gluon-gluon fusion as described in Sec. 2.3.3. Note that in all cases, the bands represent the 7-point scale variations.

As expected, the NNLO QCD corrections are rather mild, at the level of 5%, while the NLO QCD ones are larger, amounting to about 20% over a large range. The non-factorisable corrections are essentially negligible and their curve is almost indistinguishable in the ratio plot. Turning to the EW corrections, we note that, as typical for a high-energy collider such as the LHC, they grow large at high scales under the influence of Sudakov logarithms. In particular, they become as large as -5% in the invariant-mass range of about $1\,\text{TeV}$. These corrections also include the photon-induced contribution which has been singled out and found to be at the level of 1%. Interestingly, this contribution is rather constant over the entire considered phase-space region.

We now turn to a discussion of the VBF approximation. It can be seen that at low invariant masses, the VBF approximation is very close to the full computation at LO. On the other hand, at NLO QCD, the two computations can differ by up to 10% at $m_{\text{jj}} = 350\,\text{GeV}$ while converging to within a per cent above invariant masses of $700\,\text{GeV}$. Such a behaviour is due to real QCD radiation contributions for processes with hadronically decaying heavy gauge boson, in the present case $pp \rightarrow \text{H}(V \rightarrow \text{jj})$. While configurations with an invariant mass of the jets around the mass of the W or Z boson are forbidden at LO due to event selection, real radiation contributions can lift these requirements, hence making VH contributions significant. Such a pattern has been first observed for vector-boson fusion in [81,115] and for top-quark processes in [110,186].
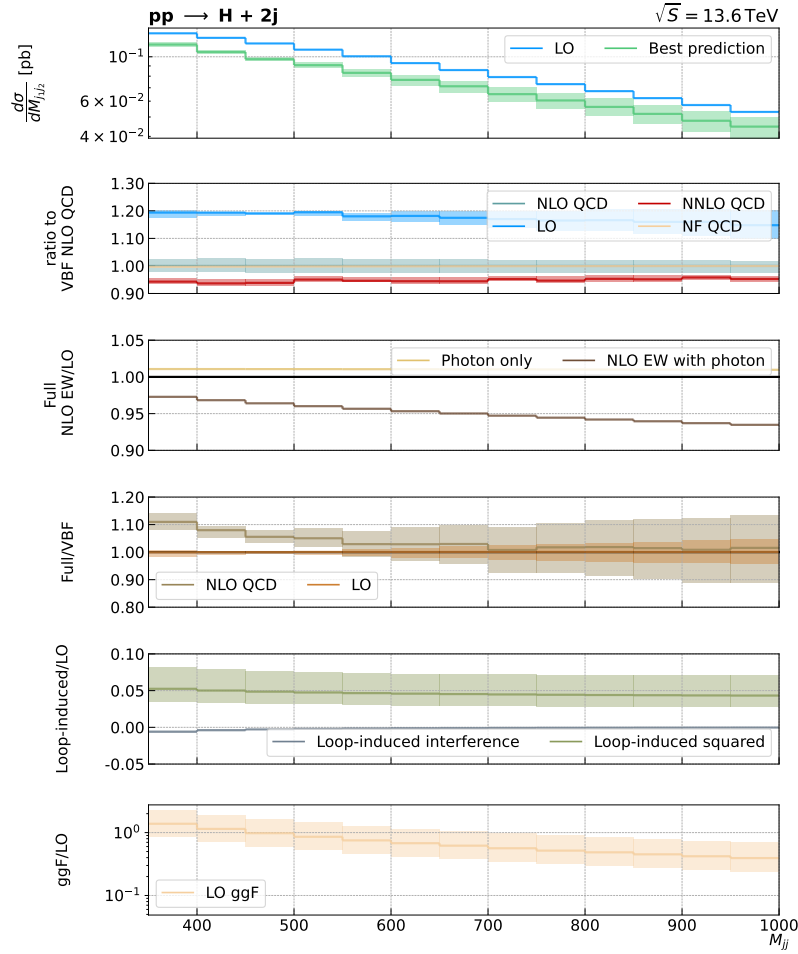
Figure 4: Differential distribution in the invariant mass of the two tagging jets for pp → Hjj at 13.6 TeV within the STXS setup Eqs. (6)–(7). See main text for more details. The bands represent the 7-point scale variations.

Finally, the interference of the EW production with the loop-induced production is essentially negligible as it is below 1% over the full range. On the other hand, the squared loop-induced contribution is reaching about 5% at $m_{jj} = 350$ GeV to stabilise slightly above 4% above invariant masses of 600 GeV. We recall that these contributions are for the quark-induced channels and constitute an irreducible contribution to the EW production pp → Hjj that will be measured experimentally if not subtracted.

In Figs. 5 and 6, the STXS observables of Ref. [6] are presented with panels for the individual types of corrections as in Fig. 4. In Fig. 5, the two-dimensional distribution in the invariant mass of the two tagging jets and their azimuthal angle difference are shown. In particular, in Fig. 5, the bins for the invariant mass of the two hardest jets below 350 GeV are displayed. This part of the phase-space is mostly dominated by VH production, justifying why no VBF predictions are provided. It is interesting to observe that QCD corrections for the bins with an invariant mass below the masses of the W/Z bosons (*i.e.* [0, 60] GeV), the QCD corrections are gigantic, being 10 to 20 times larger than the LO predictions. At LO, such phase-space regions cannot feature a resonant weak boson and therefore exhibit very low cross sections. At NLO, thanks to real radiation contributions new phase space regions are opening up, allowing the weak bosons to be resonant. The EW corrections do not show distinctive features while the photon-induced contribution remains constant in all bins. In this phase-space region, the loop-induced contributions are very much suppressed. This is not the case for the gluon-gluon
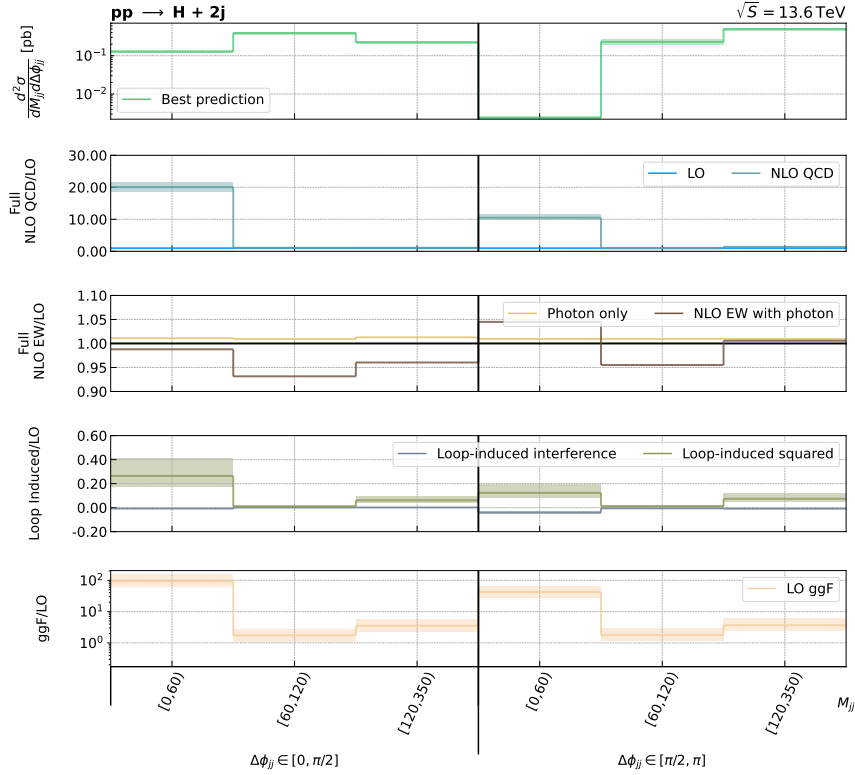
Figure 5: Multi-dimensional STXS bins for pp $\to$ Hjj at 13.6 TeV. See main text for more details.

fusion contribution which there is larger than the EW production by almost two orders of magnitude. This is simply due to the gluon luminosity at low energy at the LHC. It is worth pointing out that the STXS bins are also divided according to the transverse momentum of the Higgs boson and two jets. We have not shown this splitting here for aesthetic reasons (the bin $[25, +\infty[$ is zero at Born level) but these bins are provided in the repository. In addition to the original STXS prescription (stage 1.1), we have added two bins in $\Delta\phi_{jj}$ ($[0, \pi/2]$ and $[\pi/2, \pi]$).

In Fig. 6, the three-dimensional distribution in the invariant mass of the two tagging jets, their azimuthal angle difference, and the transverse momentum of the Higgs boson are shown. In particular, the STXS bins with $m_{jj} > 350$ GeV are shown. The QCD corrections are moderate for all bins. The photon-induced contributions stay at the per-cent level over the full range, while full EW corrections become larger negative (about -15%) with increasing invariant mass. It is worth noting that the VBF approximation reproduces the full EW production cross sections well for these bins of high-invariant jet mass at both LO and NLO QCD, apart from the bin with $m_{jj} \in [350, 700]$, $p_{T,H} > 200$ GeV, and $\Delta\phi_{jj} \in [\pi/2, \pi]$. There, the full EW contribution differs by 50% from the VBF-approximated one as in this bin a large VH contribution occurs when real radiation is present. The loop-induced contributions are also small in all considered regions. Finally, the gluon-gluon-fusion contribution is rather large in all bins, and it culminates in the bins with high transverse momentum of the Higgs boson and $\Delta\phi_{jj} \in [\pi/2, \pi]$. Again the splitting of STXS bins according to $p_{T,Hjj}$ is not shown here, but is available in the public repository of our results.
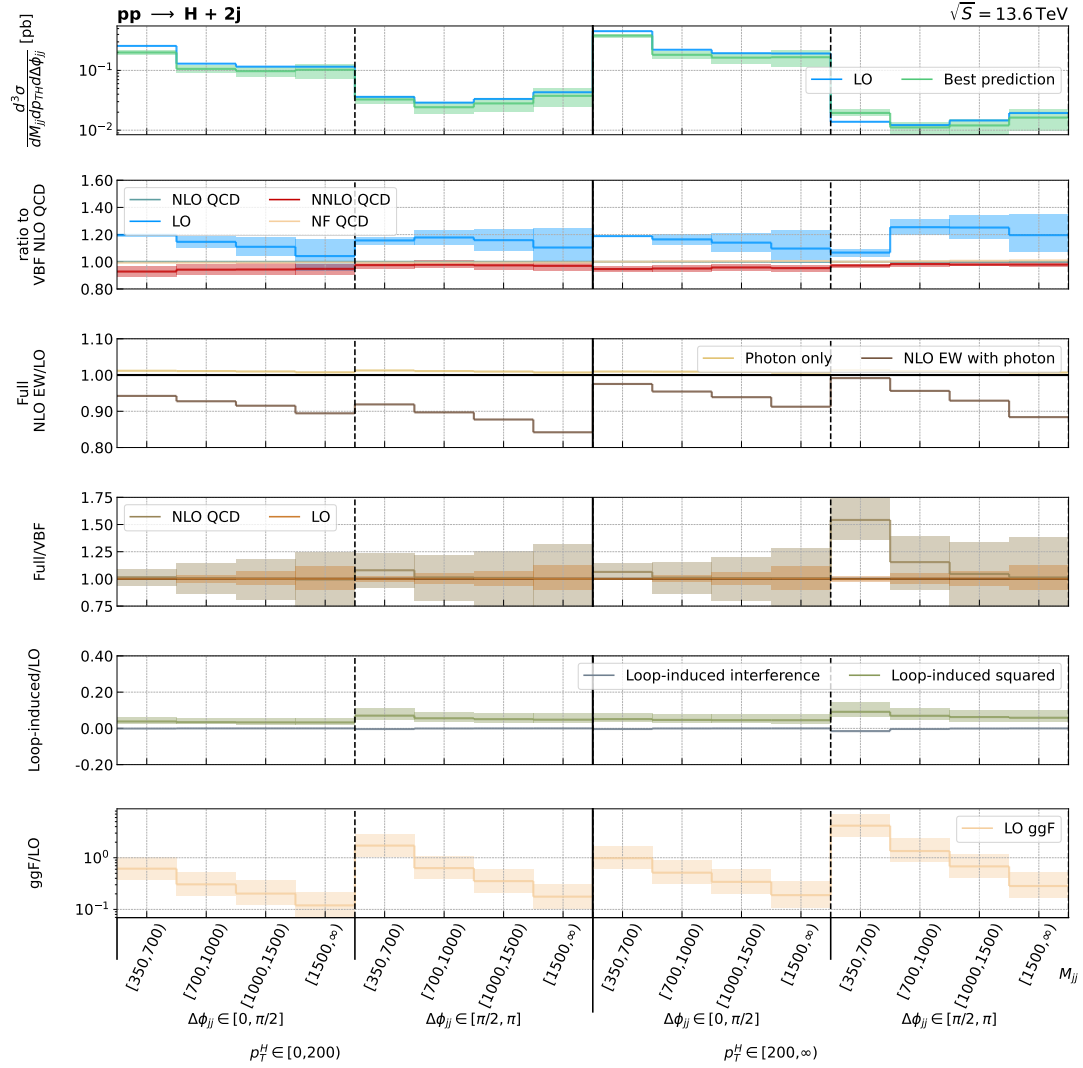
Figure 6: Multi-dimensional STXS bins for pp → Hjj at 13.6 TeV. See main text for more details.

5.2 Fiducial regions

In this section, fiducial cross sections as well as two-dimensional distributions are discussed. For the plots, the various panels show the same types of contributions as in the previous section. Given that **fiducial (a)** and **fiducial (b)** phase spaces are very similar, we here only discuss results for the former.

Cross sections First, in Table 4 we discuss the fiducial cross sections for **fiducial (a)**. In the upper part of the table, the numbers for the VBF approximation are collected. It is interesting to observe that the NLO QCD corrections are at the level of 12% while the NNLO QCD ones amount to about 25% of their size, as expected from power-counting arguments. On the other hand, the non-factorisable corrections at NNLO QCD are at the per-mille level and are therefore negligible for phenomenological considerations. In particular, while we include them in our best predictions, they actually do not play any significant role. In the second part of the table, *full* predictions in the sense that all t, u, s contributions as well as their interferences are

Table 4: Cross sections for the **fiducial (a)** phase space. The various contributions and corrections are described in detail in Sec. 2.3. The value of the best prediction is obtained from Eq. (11).

Order	σ[pb]	δ[%]
VBF approx.		
LO $[\alpha^3]$	2.479(1)	-
NLO QCD $[\alpha^3\alpha_s]$	-0.300(3)	-12.1
NNLO QCD $[\alpha^3\alpha_s^2]$	-0.088(7)	-3.55
NNLO QCD non-fact. $[\alpha^3\alpha_s^2]$	-0.0053766(7)	-0.22
Full		
LO $[\alpha^3]$	2.4772(1)	-
NLO QCD $[\alpha^3\alpha_s]$	-0.2648(10)	-10.7
NLO EW $[\alpha^4]$	-0.14759(5)	-5.95
Photon induced $[\alpha^4]$	0.021286(2)	+0.86
Loop induced int. $[\alpha^2\alpha_s^2]$	-0.003301(1)	-0.01
Loop induced squ. $[\alpha\alpha_s^4]$	0.136403(9)	5.5
LO ggF $[\alpha\alpha_s^4]$	1.7751(6)	71.5
$g\gamma \to ggH$ $[\alpha^2\alpha_s^3]$	$4.3(1) \times 10^{-6}$	0.0
Best prediction		
pp $\to$ Hjj	2.041(9)	-17.6

considered. The full LO predictions only differ insignificantly from those in the VBF approximation. The NLO QCD corrections are also of the same order in both approaches, even if the full result is slightly lower. The NLO EW corrections, including photon-induced contributions, are about -5% while the photon-induced contributions are below the per-cent level. As for the non-factorisable corrections, interference contributions between the EW production and the loop-induced ones are at the per-mile level. On the other hand, the loop-induced contributions squared, retaining only the quark channels which are therefore an irreducible background to the EW production of Hjj, are of the order of the NLO EW corrections, but exhibit an opposite sign. Considering also partonic channels with external gluons, the LO gluon-gluon fusion contribution with two identified jets is particularly large, at the level of 71%, as already observed in Ref. [5].[10] These contributions are typically not part of the signal and subtracted in experimental analyses, which makes therefore precise theoretical predictions for ggF crucial even for VBF measurements. Finally, the $g\gamma \to ggH$ process is completely negligible due to the small photon PDF and coupling factor suppression. Compared, for instance, to the related $gg \to ggH$ which is dominating the gluon-gluon fusion contribution, the $g\gamma \to ggH$ cross section comes with an extra factor of α/α_s. Due to its smallness, the $g\gamma \to ggH$ contribution is not discussed further and not shown in the differential distributions.

Differential distributions In Fig. 7, the double differential distribution in the transverse momentum of the Higgs boson and the rapidity difference of the two jets is displayed. Interestingly, NLO QCD corrections are largest for small rapidity differences of the two jets. They then tend to grow larger for larger Higgs transverse momentum. At NNLO QCD, the behaviour is opposite where the corrections tend to become smaller for larger rapidity differences.

As expected, NLO EW corrections grow negatively larger for larger transverse momentum

---

[10]Note that in Ref. [5], the ggF contribution is even dominant over the EW production given that there, no invariant-mass and rapidity-difference cuts are applied to the tagging jets.
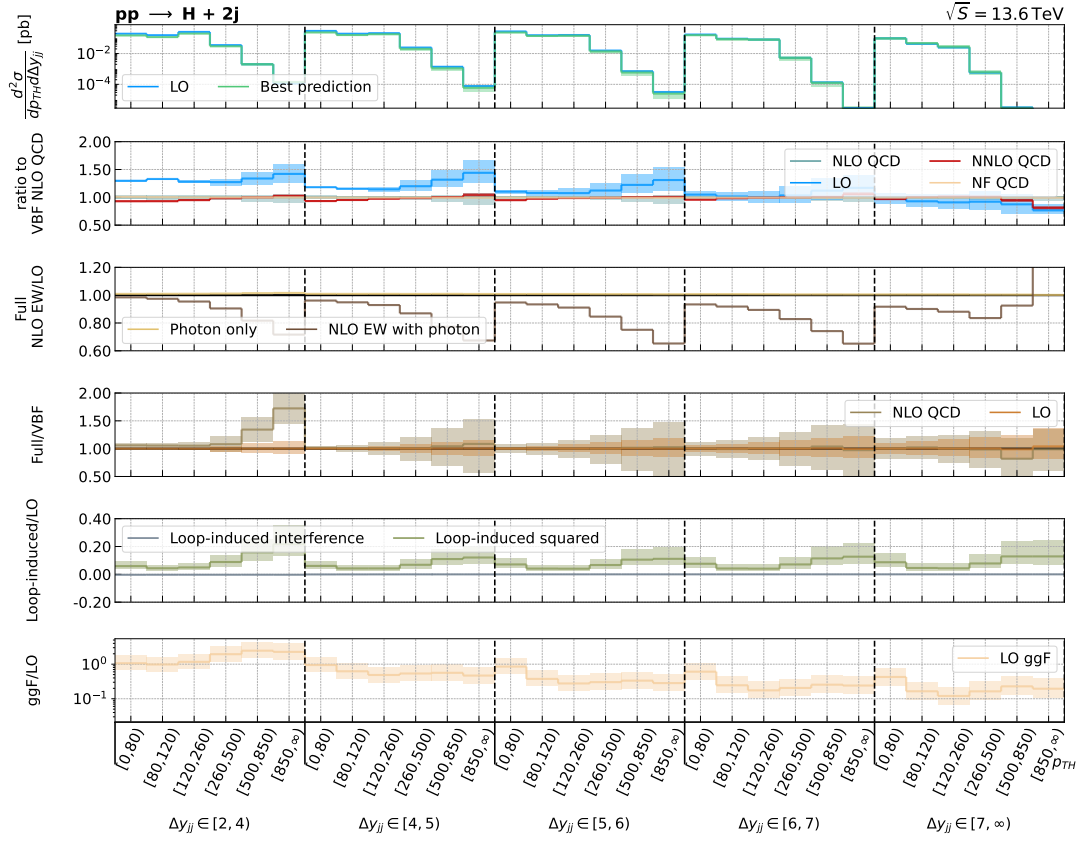
Figure 7: Differential distribution for pp → Hjj at 13.6 TeV for the **fiducial (a)** phase space for the transverse momentum of the Higgs boson and the rapidity difference of the two jets. See main text for more details.

of the Higgs boson that correspond to the high-energy limit where Sudakov logarithms become dominant. The photon-induced contribution is almost constant over the full range at the level of 1%. The two highest transverse momentum bins for $\Delta y_{jj} \in [7, \infty[$ exhibit a distinct behaviour. As these bins are highly suppressed (by several orders of magnitude), their Monte Carlo errors are very large, rendering the numbers for the EW corrections unreliable there.

As explained above, the VH contribution is sizeable when the transverse momentum of the Higgs boson is large, *i.e.* when the Higgs boson is recoiling against the two jets that are most likely to originate from the decay of a heavy gauge boson. At LO the effect is not visible due to the imposed selection cuts, but it becomes pronounced at NLO QCD with an impact reaching up to 70% in parts of phase space. This effect has already been reported in Ref. [5].

The interference of the loop-induced with the pure tree-level EW amplitude is negligible. This is not the case for the loop-induced squared contribution that can be larger than 20% of the full EW production of Hjj for large Higgs transverse momentum. In general, the latter contributions are between 5% and 10% across the phase space.

Let us now turn to Fig. 8, which shows the two-dimensional distribution in the invariant mass and the transverse momentum of the Higgs boson. As observed previously, the NLO QCD corrections are larger at large transverse momenta of the Higgs boson while the NNLO QCD ones become milder in these regions.

The EW corrections show similar features as in previous distributions. In particular, the quark-induced contributions are becoming large in the high-energy limit under the influence
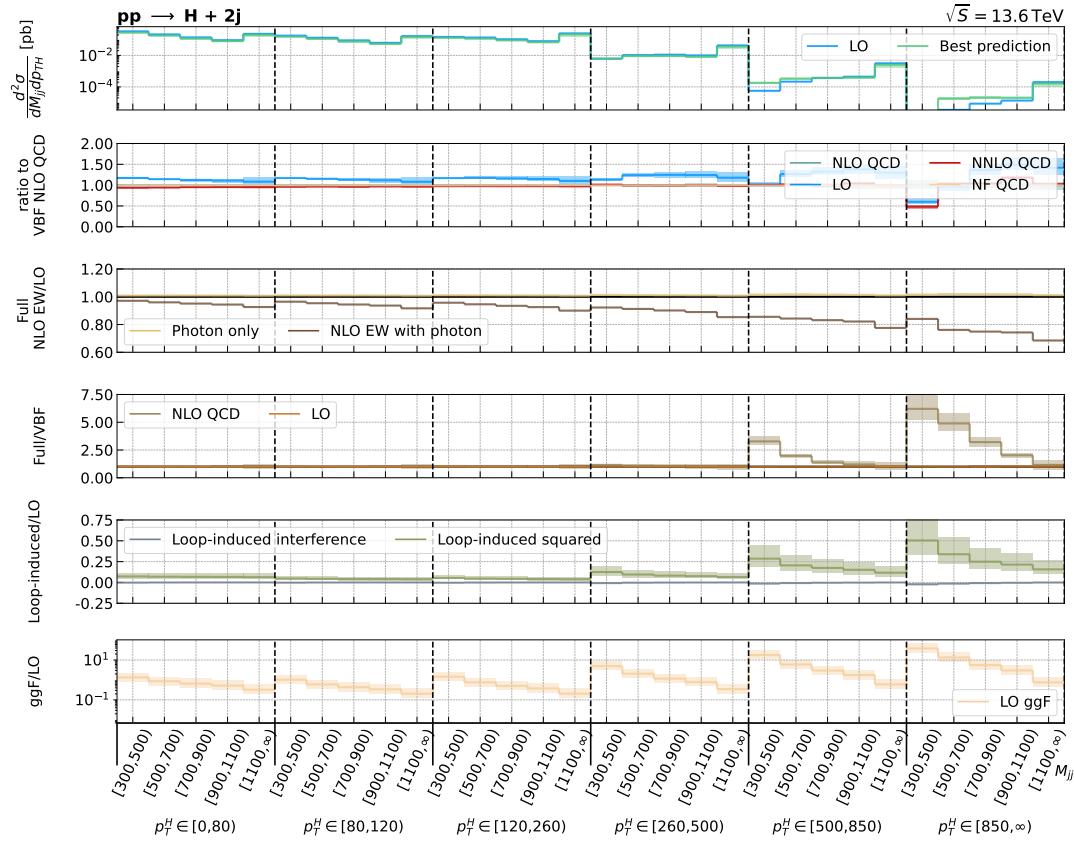
Figure 8: Differential distribution for pp → Hjj at 13.6 TeV for the **fiducial (a)** phase space for the transverse momentum of the Higgs boson and the invariant mass of the two jets. See main text for more details.

of Sudakov logarithms while the photon-induced contributions are constant throughout.

The third-to-lowest panel illustrates that the *V*H contribution is particularly enhanced for large transverse momenta of the Higgs boson due to the recoil effect described above [81,110, 115,186]. The effect can be as large as almost 600% in some bins. In the very same region the loop-induced squared contributions are also the largest.

Parton-distribution functions   Finally, given recent developments in approximate N3LO PDF sets [187–189], we have computed LO and NLO QCD predictions using the newly introduced PDF sets. The idea here is to quantify the numerical impact of the newly introduced PDF sets for a realistic experimental setup. The results are tabulated in Tables 5,6, and 7. At LO, we observe a difference of 3.4% between the nominal PDF4LHC21_40 set and the approximate N3LO PDF set [189]. The difference between the nominal PDF4LHC21_40 and the NNLO QCD set is smaller and is of 0.8%. For, NLO QCD in the full calculation, the relative corrections are essentially unchanged and amount to around −10.5% in both cases with differences at the per-mille level. The same hold true for the EW corrections and photon-induced contributions as well. For the VBF-approximated calculation, the shift at LO is at the level of 3.2%, in line with the full calculation. As in the full calculation, the NLO QCD corrections in the VBF approximation using different PDF sets are virtually identical, with differences only at the per-mille level, as shown in the Table 6. Further investigations of the interplay between approximate N3LO and fixed-order calculations are left for future work.

Table 5: Predictions at LO and NLO QCD for the full calculation for the **fiducial (a)** phase space for different PDF sets. Note that MSHT20xNNPDF40 is shorten to MSHTxNNPDF in the table.

Order	PDF4LHC21_40	MSHTxNNPDF_NNLO_qed	MSHTxNNPDF_aN3LO_qed
$\sigma_{\mathrm{LO}}^{\mathrm{Full}}[\,\mathrm{pb}]$	2.4772(1)	2.4967(1)	2.5606(1)
$\Delta_{\mathrm{NLO\,QCD}}^{\mathrm{Full}}[\,\mathrm{pb}]$	-0.2648(10)	-0.262(1)	-0.266(1)
$\delta_{\mathrm{NLO\,QCD}}^{\mathrm{Full}}[\%]$	-10.7	-10.5	-10.4

Table 6: Predictions at LO and NLO QCD for the VBF calculation for the **fiducial (a)** phase space for different PDF sets. Note that MSHT20xNNPDF40 is shorten to MSHTxNNPDF in the table.

Order	PDF4LHC21_40	MSHTxNNPDF_aN3LO_qed
$\sigma_{\mathrm{LO}}^{\mathrm{VBF}}[\,\mathrm{pb}]$	2.479(1)	2.5587(1)
$\Delta_{\mathrm{NLO\,QCD}}^{\mathrm{VBF}}[\,\mathrm{pb}]$	-0.300(3)	-0.3030(3)
$\delta_{\mathrm{NLO\,QCD}}^{\mathrm{VBF}}[\%]$	-12.1	-11.8

6 Parton shower

6.1 Comparison between fixed order and parton shower predictions for VBF

In this section, we compare the predictions obtained using the event generators described in Secs. 3.2 and 3.3. Specifically, we focus on the **fiducial (b)** phase space region defined in Sec. 4.2. Results for the **fiducial (a)** region have similar behaviour.

We compare NLO QCD (violet), NNLO QCD (red) and NLOPS (green) predictions for both inclusive (Figs. 9 and 10) and exclusive (Fig. 11) observables for illustration. As done in the previous sections, the theoretical uncertainty associated with NLO and NNLO QCD calculations is represented by a solid band corresponding to the scale variations (dubbed *ME scale* in the legend).

At NLOPS, as our reference we use the VBF POWHEG-BOX implementation [79] showered with PYTHIA 8 using a dipole recoil and the option POWHEG:pThard = 0. For this prediction, we show again the scale variations in the hard matrix element (green solid band). The total scale uncertainty associated with the reference NLOPS generator also comprises the uncertainty stemming from the choice of the hard scale in the parton shower evolution (see Sec. 3.2.2), which we vary by using the POWHEG:pThard = 2 option. This uncertainty is given by the hatched band labelled *ME + PS starting scale*. Finally, the total uncertainty of the NLOPS prediction also includes the envelope of all the NLOPS generators considered in this study (scale + PS scheme). The breakdown into several NLOPS generators, including shower starting scale for the reference prediction (dashed green line), is shown in the bottom panel.

In Fig. 9, we show the dijet invariant mass M_{jj}, requiring a small ($p_{\mathrm{T,H}} < 80$ GeV, left) and a moderate (80 GeV $< p_{\mathrm{T,H}} < 120$ GeV, right) Higgs transverse momentum. In Fig. 10, we instead show the dijet invariant mass requiring a moderate ($2 < |\Delta y_{\mathrm{jj}}| < 4$, left) and a large ($4 < |\Delta y_{\mathrm{jj}}| < 5$, right) dijet rapidity separation. The dijet invariant mass, Higgs transverse momentum, and the dijet rapidity separation are standard inclusive observables for VBF-like processes, meaning that we expect a good description from the fixed-order predictions. Since these observables involve jet reconstruction (directly or through the application of jet-selection cuts), the parton showering will also affect the predictions. We find that in general the central NLOPS predictions lie between the NLO and the NNLO QCD ones.

Table 7: Predictions at LO and NLO EW for the full calculation for the **fiducial (a)** phase space for different PDF sets. The photon-induced contribution is singled out. Note that `MSHT20xNNPDF40` is shorten to `MSHTxNNPDF` in the table.

Order	PDF4LHC21_40	MSHTxNNPDF_NNLO_qed	MSHTxNNPDF_aN3LO_qed
$\sigma_{\text{LO}}^{\text{Full}}[\text{pb}]$	2.4772(1)	2.4967(1)	2.5606(1)
$\Delta_{\text{NLO EW}}^{\text{Full}}[\text{pb}]$	-0.14759(5)	-0.14826(3)	-0.15238(3)
$\delta_{\text{NLO EW}}^{\text{Full}}[\%]$	-5.95	-5.94	-5.95
$\Delta_{\gamma}^{\text{Full}}[\text{pb}]$	0.021286(2)	0.021453(2)	0.021887(2)
$\delta_{\gamma}^{\text{Full}}[\%]$	+0.86	+0.86	+0.85

Furthermore, the central NNLO QCD predictions lie within the total uncertainty band around the NLOPS central prediction. The only exception is the lowest M_{jj} bin in the presence of a boosted Higgs (right panel of Figs. 9) or for very large dijet separation (right panel of Fig. 10). This behaviour was also observed in Ref. [5].

The NNLO uncertainty is of the order of 2%, while the NLO one is roughly twice as large. The NLOPS uncertainty estimated by varying the matrix-element and shower starting scales is smaller than the corresponding NLO theoretical uncertainty. However, once the variation of the NLOPS generator is included, the two uncertainties become comparable. This indicates that only varying the parameters within a single shower algorithm may yield an underestimate of the true perturbative uncertainty.

We now consider distributions that are more sensitive to the presence of additional radiation in the final state. In Fig. 11, we illustrate the transverse momentum of the Higgs boson requiring exactly two (left panel) or three (right panel) reconstructed jets. The first distribution can still be considered inclusive, as it is well defined at LO, whereas the second is exclusive, requiring the presence of an additional radiation jet. Both distributions develop terms enhanced by large logarithms $L = \log(p_{\text{T,H}}/p_{\text{T,j}}^{\min})$ at all-orders in α_s. Thus, when $\alpha_s L^2 \approx 1$, *i.e.* around $p_{\text{T,H}} = 500\,\text{GeV}$, the accuracy of the fixed-order prediction is lost. The distribution in the left panel is of particular interest given the proposal in Ref. [5] of introducing a jet veto procedure in order to reduce the contamination from the gluon-fusion background. In the region with $p_{T,H} \ll 500$ GeV, (N)NLO calculations still retain (N)NLO accuracy. We notice that NLOPS predictions overshoot both the NLO and the NNLO QCD results, but for boosted-Higgs topologies, the NLOPS curve tends to be closer to the NNLO than the NLO one. We also observe that requiring only 2 jets leads to a larger scale uncertainty, reaching 20% in the hard tail. In this case, the NLOPS uncertainty is much smaller than the NLO one, but much bigger than the NNLO one. This is somewhat expected, given the sensitivity to additional radiations. It is also worth noting that in the last bin, sensitive to all-orders corrections that can be much bigger than the nominal NNLO prediction, the error band of the fixed-order calculation clearly does not reflect the true uncertainty.

As expected, requiring 3 jets (right panel of Fig. 11) is even more sensitive to the radiation pattern provided by the showers. In the region with $p_{T,H} \ll 500$ GeV, (N)NLO calculations only retain (N)LO accuracy. In this case, parton shower uncertainties are again of the order of 20%, and they are of the same order as the NNLO ones for small-moderate $p_{\text{T,H}}$ while for a boosted Higgs the NNLO uncertainty substantially increases. It is worth noting that the NLOPS prediction is in agreement with the NNLO QCD curve, but not with the NLO QCD one.

6.2 VH interference effects

In Sec. 6.1 we have considered QCD corrections to the pure VBF process. It is, however, interesting to scrutinise the full EW H+2jets production (that we shorten as Hjj),
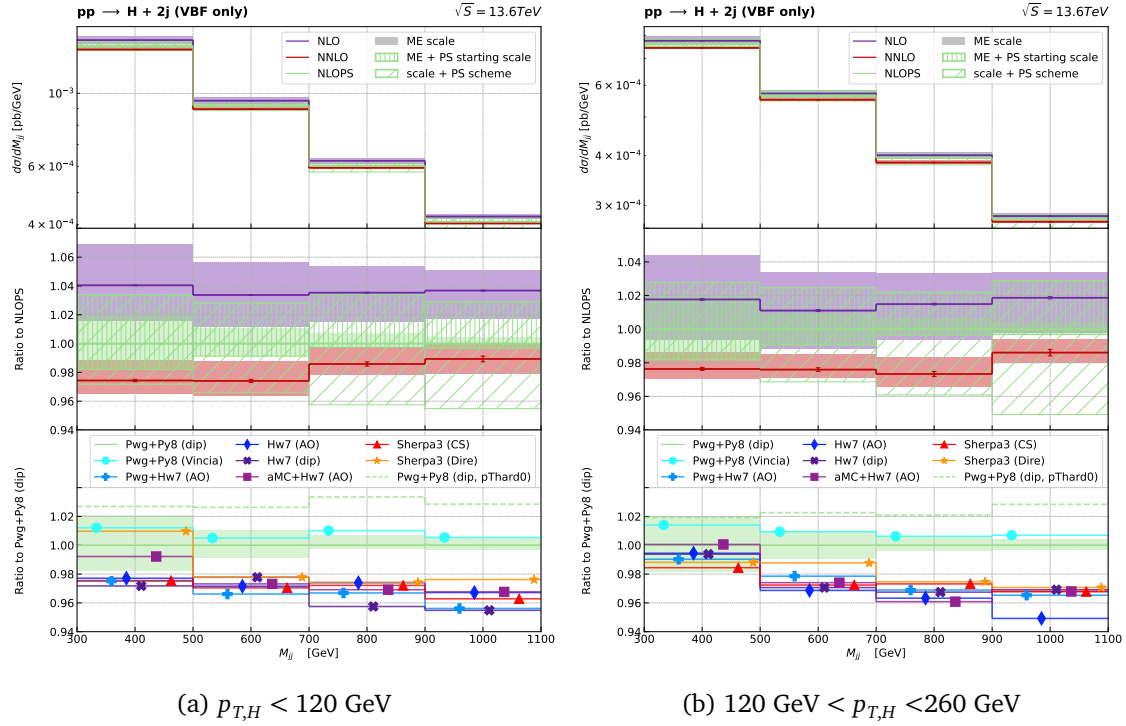
Figure 9: Fixed-order (NNLO and NLO) and NLOPS predictions within the VBF approximation for the dijet invariant mass within the **fiducial (b)** phase space, in two regions of Higgs transverse momentum. The solid bands represent the 7-point variation of the factorisation and renormalisation scales in the hard matrix elements, while for the vertical hashed green bands additionally the shower starting scale of the reference generator is varied. For the total NLOPS uncertainty, shown as diagonal hashed green bands, the scale variation and generator uncertainties are combined as detailed in our recommendations in Sec. 6.3.3. The middle panels illustrate the ratio between the respective fixed-order and the central NLOPS predictions. The lower panels show the spread of the predictions obtained with the various NLOPS generators considered in this study.

which comprises both the VBF and the VH production modes. For this study we choose three predictions, representative of the various parton showers and matching schemes, namely POWHEG-BOX+PYTHIA 8 (simple shower with dipole recoil, in green), MAD-GRAPH5_AMC@NLO+HERWIG 7 (angular-ordered shower, in violet), and SHERPA 3 (CS shower, in red).

In particular, Fig. 12 illustrates the dijet invariant mass within the same cuts as Fig. 10 for these three NLOPS predictions, including the uncertainty stemming from the renormalisation and factorisation scale variations in the hard matrix element, for the pure VBF contribution (solid line and band), and the full EW Hjj production (dashed lines and hatched bands). As expected, for a moderate Δy_{jj} separation (left plot), the Hjj prediction is roughly $5-8\%$ larger the pure VBF one across our generators (ratio plot in the last panel), and uncertainties stemming from the hard matrix elements scale variations are roughly $4-5\%$.

Requiring $\Delta y_{jj} > 4$ (right) strongly suppresses the VH contribution, and the ratio between Hjj and VBF is much closer to 1, with differences at most of 2% in the lowest M_{jj} bins. However, while we notice that for the POWHEG-BOX+PYTHIA 8 and MADGRAPH5_AMC@NLO+HERWIG 7 generators, both the central values and the scale variations are similar between VBF and Hjj, for SHERPA 3 this is true only for the central value, while scale variations appear much larger.

(a) $2 < |\Delta y_{jj}| < 4$.

(b) $4 < |\Delta y_{jj}| < 5$.
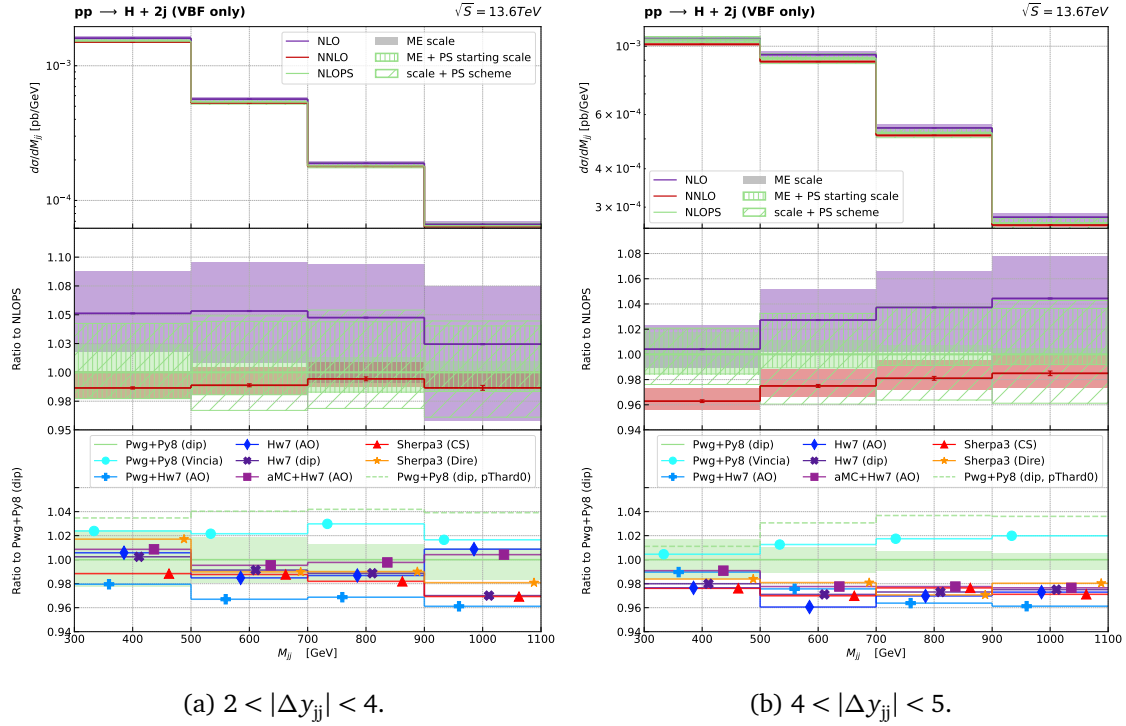
Figure 10: As in Fig. 9, but for two regions of dijet rapidity separation.

As expected, the differences between the pure VBF sample and the full EW Hjj one are very similar across all the NLOPS samples.

6.3 Considerations on parton shower and matching uncertainties

As discussed in Sec. 2.2, parton shower and matching uncertainties amount to a sizeable contribution to the error budget of differential distributions. Given the need for a coherent path for understanding and reducing such systematics, we provide here a recommendation for a robust assessment of parton shower and matching uncertainties, given the current state of the art.

To derive this recommendation we focus on the figures shown in Sec. 6.1, but our considerations holds for all the distributions of the present study.

6.3.1 Uncertainties from varying NLOPS generators

From the middle panel of Figs. 9, 10, and 11, it is evident that the error obtained by simply performing a scale variation on a single NLOPS sample (ME + PS starting scale) must be combined with the uncertainty arising from variations in matching and parton-shower schemes. It is also evident that the largest uncertainty stems from varying the parton shower, rather than the matching scheme. This was already observed, *e.g.* in Ref. [5]. In the bottom panels, we illustrate the breakdown of all the predictions contributing to this envelope. For inclusive distributions (such as those in Figs. 9, 10 and the left panel of Fig. 11), HERWIG 7 and SHERPA 3 predictions are rather close to each other, while the PYTHIA 8 showers always yield higher rates. Looking at more exclusive observables (such as the right panel of Fig. 11), *i.e.* those that can be defined only if a third jet is present, again all the SHERPA 3 and HERWIG 7 predictions appear quite close to each other. Within the group of these neighbouring predictions, the most different is typically the HERWIG 7 angular-ordered shower with internal matching which has

(a) Two reconstructed jets.   (b) Three reconstructed jets.
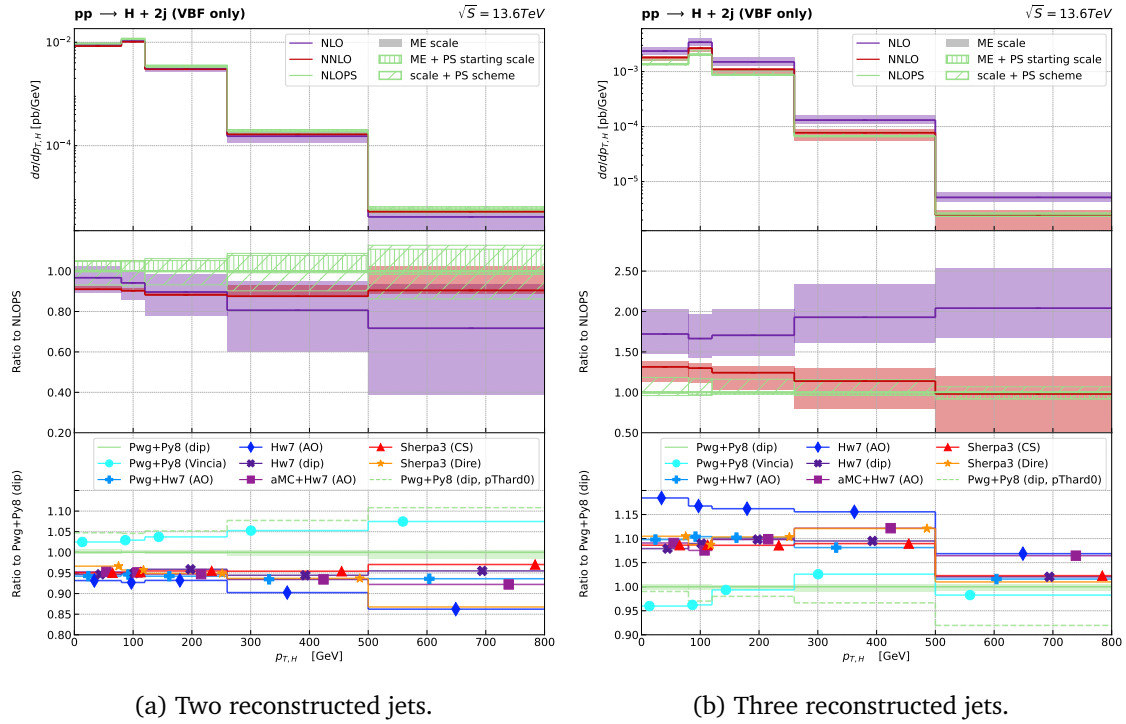
Figure 11: Higgs transverse momentum within the **fiducial (b)** phase space region, requiring exactly two (left) or three (right) reconstructed jets. The naming of the curves is the same as in Fig. 9.

a higher rate by up to 10%. Both PYTHIA 8 curves instead undershoot the SHERPA 3/HERWIG 7 envelope by roughly 10%.

In general, there is a remarkably good agreement between HERWIG 7 and SHERPA 3, regardless of the shower and the matching used, with at most 5% discrepancies for inclusive observables, and at most 10% differences for more exclusive ones. PYTHIA 8 predictions are somehow always outliers, with the default "simple" shower with dipole recoil and default hard scale setting being the closest to HERWIG 7 and SHERPA 3.

6.3.2 Scale uncertainties in a NLOPS simulation

We now comment on scale variations in the parton showers. For all generators used in this study, the structure of higher-order corrections to soft-gluon emission [190] was used to deduce the functional form of the argument of the strong coupling. The renormalisation scale is therefore proportional to the transverse momentum of the emission, although the precise kinematical definition of the transverse momentum can differ among the codes. Variations of this scale are partially compensated by higher-order corrections that (at NLL) affect the soft emissions due to the combined structure of the leading poles and leading logarithms [191–196]. The parton showers considered in this study generally have LL accuracy, with some NLL violating terms arising either from the inability to describe non-global observables (as is the case for the angular-ordered shower [197]) or from the handling of multiple emissions at commensurate hardness (see *e.g.* Refs. [84,198] for a detailed discussion). However, all of the parton showers implement splitting functions compatible with NLL evolution, such that the NLL renormalisation scale variations can be used. The uncertainty stemming from NLL-violating terms is of kinematical origin and should be parametrised in different way, for example by varying the recoil scheme.

(a) $2 < |\Delta y_{jj}| < 4$.   (b) $4 < |\Delta y_{jj}| < 5$.
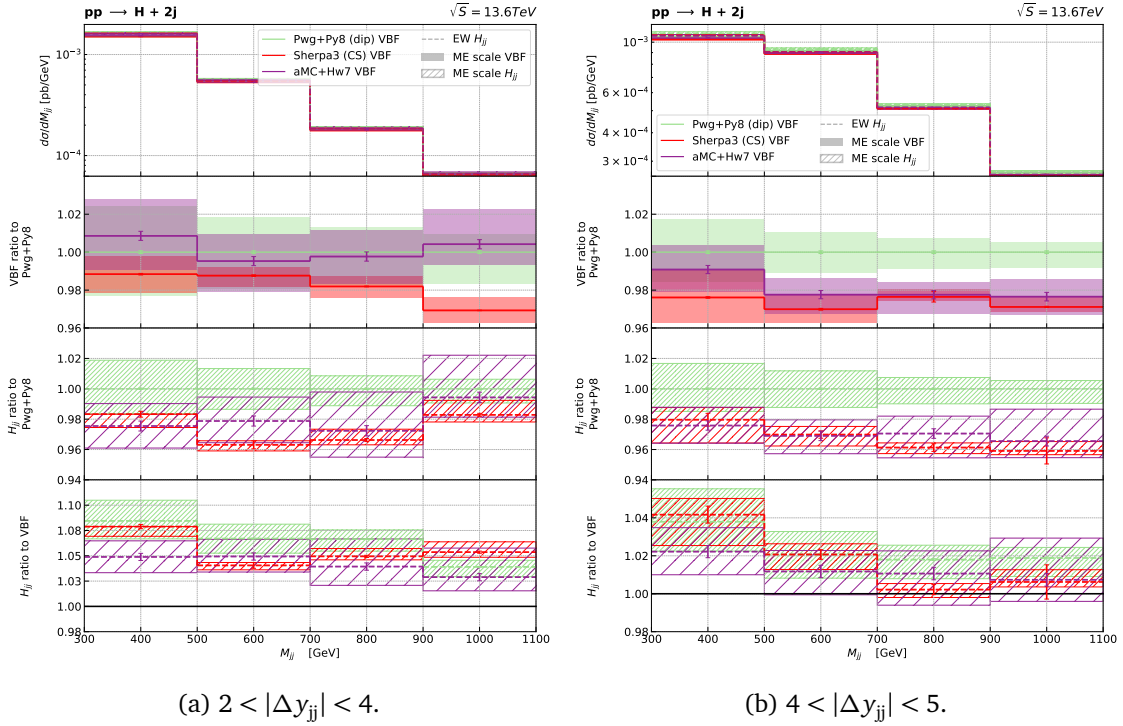
Figure 12: Dijet invariant mass distributions at NLOPS, considering the full EW Hjj production mode (dashed lines) and just the pure VBF contributions (solid lines) for a representative PYTHIA 8 (green), SHERPA 3 (red), and HERWIG 7 (violet) prediction, for two regions of dijet rapidity separation in the fiducial phase space **fiducial (b)**. The solid (hatched) bands represent the uncertainty stemming from the 7-point scale variation in the hard matrix element calculations of the VBF (EW H + 2 jets) production mode. The second (third) panel illustrates the ratio with respect to the central PYTHIA 8 prediction for the VBF (Hjj) production mode. The fourth panel illustrates the ratio between the Hjj predictions with respect to the central VBF one for each NLOPS generator.

At NLL, the higher-order corrections proportional to the QCD beta function can be implemented as a term multiplying only soft emissions [183]. More specifically, if we wish to vary the argument of the running coupling by a factor r, the following functional form of the coupling should be used:

$$\alpha_s(rk_t) \to \alpha_s(rk_t)\left[1 + f(z)\frac{\alpha_s(rk_t)}{2\pi}\beta_0 \ln r^2\right], \tag{13}$$

where β_0 is the one-loop QCD beta function, and $f(z) = 1$ when the emission is soft, and $f(z) = 0$ otherwise. PYTHIA 8 is the only tool which implements this type of NLL-preserving scale variations in its current public version [199]. The HERWIG 7 shower implements Eq. (13) with $f(z) = 0$, consistent with LL evolution but not with NLL. The current public version of SHERPA's CS shower sets $f(z) = 1$ by default, alternatively the LL correct $f(z) = 0$ can be used. For the purpose of this study, we have modified the SHERPA 3 generator to also include NLL scale variations.[11] We note that the DIRE parton shower use separate α_s schemes for the soft and collinear part of the splitting functions, and the ALARIC parton shower treats soft and collinear terms as separate splitting kernels [200]. In both cases the NLL scale variation is implemented. In the case of POWHEG matching, we should also consider scale variations

---

[11]This option will be part of SHERPA 3 releases starting from version 3.1.

(a) $2 < |\Delta y_{jj}| < 4$.   (b) $4 < |\Delta y_{jj}| < 5$.
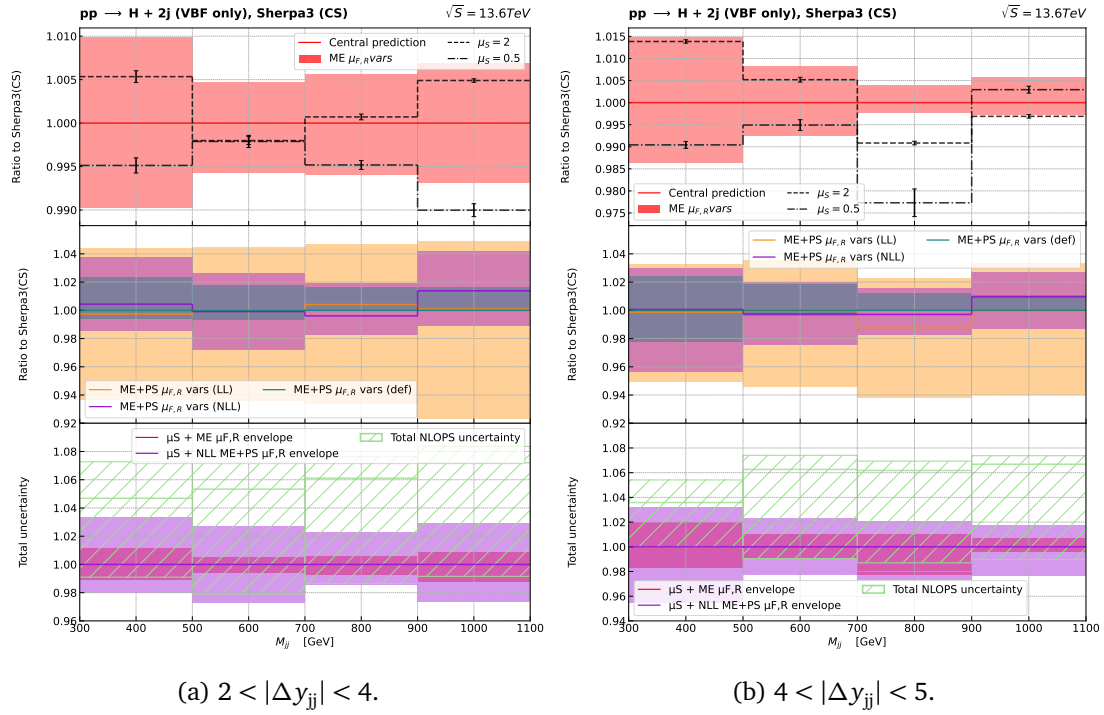
Figure 13: Relative uncertainty for the dijet mass distributions at NLOPS for the SHERPA 3 default shower, breaking into two dijet rapidity separation Δy_{jj} regions. Fiducial cuts are the same as in Fig. 10.

in the hardest emission generator. However at present no variation of this kind is possible in the POWHEG-BOX, which only allows for renormalisation and factorisation scale variations entering the NLO normalisation of the event.

Factorisation scale variations are currently possible only in SHERPA 3 (on-the-fly) [201] and HERWIG 7. They will become available in PYTHIA 8 starting from release 8.316.

The result for the M_{jj} distribution, broken into two Δy_{jj} ranges, is shown in Fig. 13. All curves are normalised with respect to the central prediction (CS shower), so to better assess the size of the relative uncertainties. In the first panel, we show the uncertainty from scale variations in the matrix element (red solid band) and from varying the shower starting scale of a factor 2 up (dashed black line) and down (dash dotted line). In the second panel, we compare the band stemming from renormalisation and factorisation scale variations not only in the matrix element but also including a correlated variation in the shower splitting kernels, using the default option (renormalisation scale compensating term always present, in green), the one compatible with NLL evolution (renormalisation scale compensating term present only for soft emissions, as in PYTHIA 8, violet) and the one compatible with LL evolution (compensating term never present, as in HERWIG 7, orange). From the first panel, we see the scale variatiions in the pure matrix element is of the order of 1% up and down, while the NLL variation is roughly 2-3 times bigger. The default SHERPA 3 variation obtained is of the order of 1-2%, and thus often underestimates the NLL one, while the LL variation yields a much band with spread of around 10%. In the bottom panel we sum in quadrature the uncertainty coming from the parton shower starting scale together with the factorisation and renormalisation scale variation in the matrix element (red) or in the matrix element and in the shower using the NLL prescription for the renormalisation scale (violet). The NLL (LL) band is smaller (comparable) in size with the one obtaining from the envelope of all NLOPS generators (bottom panel of Fig. 10), which dominates the NLOPS uncertaintes as computed in the previous sections,

represented by the green band in the bottom panel of Fig. 13. Thus we believe that comparing different tools with the same formal accuracy has always to be performed. However, in view of more accurate parton showers algorithms being developed, we encourage the authors of all the tools presented in this study to include an option for on-the-fly factorisation scale variation, and one for both LL and NLL renormalisation scale variations.

6.3.3 Recommendations for NLOPS uncertainty estimates

Based on these observations, we propose the following recommendation for a more robust estimation of NLOPS uncertainty, which comprises both the matching and the shower variations:

1. Generate (at least) three predictions:

   – one with POWHEG-BOX and any PYTHIA 8 shower;
   – one with any HERWIG 7 shower;[12]
   – one with any SHERPA 3 shower.

   Make sure that at least one of these prediction is based on POWHEG matching, and one on MC@NLO matching.[13] Then, construct an envelope[14] out of these predictions.

2. For one of the curves computed in step 1:

   – compute a shower starting scale variation band (or a `pThard` variation in the context of POWHEG-BOX +PYTHIA 8 matching);
   – compute the renormalisation and factorisation scale variation band, possibly including also scale variations in the shower.

   Sum these bands in quadrature and combine this uncertainty in quadrature with the first envelope uncertainty.

Notice that, contrary to what is done in many experimental analyses, we do not distinguish between matching and parton-shower uncertainties, but rather provide a unified band, because the two aspects are often correlated, *i.e.* a matching procedure is usually tailored to the parton shower it is applied to.

We want to remind the reader that our recommendation is based on the fact that all currently available showers that can be matched with NLO QCD calculations for VBF have the same leading-logarithmic accuracy.[15] Consequently, the predictions are equivalent, and their spread provides a genuine measure of the systematic error. This approach may need revision when NLL showers matched to NLO calculations become publicly available in fully-fledged GPMC generators. This would also imply the use of NLL scale variations.

We finally emphasise that the present study addresses only perturbative uncertainties. However, comparing three different GPMC generators — PYTHIA 8, SHERPA 3, and HERWIG 7

---

[12]Preferably with matching achieved through MATCHBOX, to ensure proper alignment of parameters between the hardest emission and parton shower generation.

[13]We remind the reader that the preferred matching scheme of SHERPA 3 is MC@NLO, for VBF in PYTHIA 8 only matching via POWHEG-BOX is allowed, while for HERWIG 7 all matching schemes are available.

[14]For inclusive distributions, since HERWIG 7 and SHERPA 3 yield similar results, one of these curves can be omitted. However, we recommend verifying this similarity for more exclusive observables.

[15]An exception is the default PYTHIA 8 shower with global recoil, which violates color coherence and should be avoided. For this reason this shower is not considered in this study.

— which implement distinct soft physics models (*e.g.* hadronisation and multi-parton interactions) while aligning all input parameters related to the hard processes as done here, should offer a reasonably robust assessment of non-perturbative uncertainties as well. A more detailed analysis of such uncertainties lies beyond the scope of this work.

7 Summary

The production of Higgs bosons via vector-boson fusion (VBF) is one of the primary Higgs-boson production mechanisms at the LHC. In this context, current investigations of Higgs-boson physics necessitate a deeper exploration of this channel. Precise and reliable theoretical predictions are therefore essential to fully exploit the potential of experimental data.

In this work, we first reviewed past experimental and theoretical studies on VBF at the LHC. This summary, particularly the accompanying tables, aims to facilitate the proper citation of VBF studies, especially of theoretical work. Additionally, we have provided theoretical predictions at fixed order and with parton-shower corrections in generic fiducial phase space regions, as well as within the STXS framework.

Regarding fixed-order predictions, we have discussed in detail all contributions to the process pp → Hjj. The contributions concerning VBF production have been calculated with state-of-the-art accuracy while the background contributions have been provided for reference only and hence with lower accuracy. The results are presented in the form of cross sections and differential distributions.

We performed a detailed comparison of different state-of-the-art NLOPS predictions, for both the VBF channel as well as the full EW Hjj production. This enabled us to formulate a prescription for assessing the theory uncertaintes: one should consider three-points variation (SHERPA 3, PYTHIA 8, HERWIG 7) and include consistently factorisation-, renormalisation-, and starting-scale variations. While we focused mostly on the VBF fiducial phase space region, we believe similar prescriptions can be a solid way of assessing NLOPS uncertainties for more generic processes.

With this work, we have gained a better understanding of current theory uncertainties for VBF production at the LHC bearing in mind the current available theoretical calculations. These findings are expected to be of great use during the run III of the LHC, where dedicated VBF measurements are foreseen. Since in our study we mainly focused on the signal process, we believe a similar collective effort is also required to get a clearer understanding of background contamination in VBF phase space regions with state-of-the-art predictions [202].

Finally, we recall that all the results and auxiliary data files can be publicly accessed at:

https://gitlab.cern.ch/LHCHIGGSXS/LHCHXSWG1/VBFStudyYR5.

We hope that this work will be useful to the community, ease the acknowledgement of theoretical contributions as well as enable the optimal use of state-of-the-art theoretical predictions in experimental analyses. In doing so, it will support further investigations of Higgs boson production via the VBF channel at the LHC.

Acknowledgments

The authors are grateful to the LHC Higgs Cross Section Working Group for providing such a framework and support for the present work. We want to thank Joey Huston and Simon Plätzer for useful discussions. This work has also greatly benefited from the PhysTeV workshop 2023 at Les Houches, France [203].

Funding information This research was supported by FermiForward Discovery Group, LLC under Contract No. 89243024CSC000002 with the U.S. Department of Energy, Office of Science, Office of High Energy Physics. BJ, MP, and SR acknowledge support by the state of Baden-Württemberg through bwHPC and the German Research Foundation (DFG) through grant No. INST 39/963-1 FUGG (bwForCluster NEMO). MP acknowledges support by the DFG through the Research Training Group RTG2044. CTP thanks the PLEIADES HPC team at the University of Wuppertal, supported by the DFG through grant No. INST 218/78-1 FUGG and the Bundesministerium für Bildung und Forschung (BMBF). DR acknowledges support by the European Union under the HORIZON program in Marie Skłodowska-Curie project No. 101153541. MZ acknowledges the financial support by the MUR (Italy), with funds of the European Union (NextGenerationEU), through the PRIN2022 grant 2022EZ3S3F.

References

[1] D. de Florian et al., *Handbook of LHC Higgs cross sections: 4. Deciphering the nature of the Higgs sector*, CERN, Geneva, Switzerland, ISBN 9789290834427 (2017), doi:10.23731/CYRM-2017-002.

[2] A. Karlberg et al., *Ad interim recommendations for the Higgs boson production cross sections at $\sqrt{s} = 13.6$ TeV*, (arXiv preprint) doi:10.48550/arXiv.2402.09955.

[3] B. Jäger, A. Karlberg, S. Plätzer, J. Scheller and M. Zaro, *Parton-shower effects in Higgs production via vector-boson fusion*, Eur. Phys. J. C **80**, 756 (2020), doi:10.1140/epjc/s10052-020-8326-7 [preprint doi:10.48550/arXiv.2003.12435].

[4] S. Höche, S. Mrenna, S. Payne, C. T. Preuss and P. Skands, *A study of QCD radiation in VBF Higgs production with Vincia and Pythia*, SciPost Phys. **12**, 010 (2022), doi:10.21468/SciPostPhys.12.1.010 [preprint doi:10.48550/arXiv.2106.10987].

[5] A. Buckley et al., *A comparative study of Higgs boson production from vector-boson fusion*, J. High Energy Phys. **11**, 108 (2021), doi:10.1007/JHEP11(2021)108 [preprint doi:10.48550/arXiv.2105.11399].

[6] N. Berger et al., *Simplified template cross sections – stage 1.1 and 1.2*, (arXiv preprint) doi:10.48550/arXiv.1906.02754.

[7] C. Bierlich et al., *Robust independent validation of experiment and theory: Rivet version 3*, SciPost Phys. **8**, 026 (2020), doi:10.21468/SciPostPhys.8.2.026 [preprint doi:10.48550/arXiv.1912.05451].

[8] T. Melia, K. Melnikov, R. Röntsch and G. Zanderighi, *Next-to-leading order QCD predictions for W^+W^+jj production at the LHC*, J. High Energy Phys. **12**, 053 (2010), doi:10.1007/JHEP12(2010)053 [preprint doi:10.48550/arXiv.1007.5313].

[9] A. Denner, L. Hošeková and S. Kallweit, *Next-to-leading order QCD corrections to W^+W^+jj production in vector-boson fusion at the LHC*, Phys. Rev. D **86**, 114014 (2012), doi:10.1103/PhysRevD.86.114014 [preprint doi:10.48550/arXiv.1209.2389].

[10] ATLAS collaboration: G. Aad et al., *A detailed map of Higgs boson interactions by the ATLAS experiment ten years after the discovery*, Nature **607**, 52 (2022), doi:10.1038/s41586-022-04893-w [preprint doi:10.48550/arXiv.2207.00092].

[11] CMS collaboration: A. Tumasyan et al., *A portrait of the Higgs boson by the CMS experiment ten years after the discovery*, Nature **607**, 60 (2022), doi:10.1038/s41586-022-04892-x [preprint doi:10.48550/arXiv.2207.00043].

[12] CMS collaboration: A. Tumasyan et al., *Measurements of Higgs boson production in the decay channel with a pair of τ leptons in proton-proton collisions at $\sqrt{s} = 13$ TeV*, Eur. Phys. J. C **83**, 562 (2023), doi:10.1140/epjc/s10052-023-11452-8 [preprint doi:10.48550/arXiv.2204.12957].

[13] ATLAS collaboration: G. Aad et al., *Differential cross-section measurements of Higgs boson production in the $H \rightarrow \tau^+\tau^-$ decay channel in pp collisions at $\sqrt{s} = 13$ TeV with the ATLAS detector*, J. High Energy Phys. **03**, 010 (2025), doi:10.1007/JHEP03(2025)010 [preprint doi:10.48550/arXiv.2407.16320].

[14] CMS collaboration: A. Tumasyan et al., *Measurements of the Higgs boson production cross section and couplings in the W boson pair decay channel in proton-proton collisions at $\sqrt{s} = 13$ TeV*, Eur. Phys. J. C **83**, 667 (2023), doi:10.1140/epjc/s10052-023-11632-6 [preprint doi:10.48550/arXiv.2206.09466].

[15] ATLAS collaboration: G. Aad et al., *Measurements of Higgs boson production by gluon-gluon fusion and vector-boson fusion using $H \rightarrow WW^* \rightarrow e\nu\mu\nu$ decays in pp collisions at $\sqrt{s} = 13$ TeV with with the ATLAS detector*, Phys. Rev. D **108**, 032005 (2023), doi:10.1103/PhysRevD.108.032005 [preprint doi:10.48550/arXiv.2207.00338].

[16] CMS collaboration: A. M. Sirunyan et al., *Measurements of Higgs boson production cross sections and couplings in the diphoton decay channel at $\sqrt{s} = 13$ TeV*, J. High Energy Phys. **07**, 027 (2021), doi:10.1007/JHEP07(2021)027 [preprint doi:10.48550/arXiv.2103.06956].

[17] ATLAS collaboration: G. Aad, *Measurement of the properties of Higgs boson production at $\sqrt{s} = 13$ TeV in the $H \rightarrow \gamma\gamma$ channel using 139 fb^{-1} of pp collision data with the ATLAS experiment*, J. High Energy Phys. **07**, 088 (2023), doi:10.1007/JHEP07(2023)088 [preprint doi:10.48550/arXiv.2207.00348].

[18] CMS collaboration: A. Hayrapetyan et al., *Measurement of the Higgs boson production via vector boson fusion and its decay into bottom quarks in proton-proton collisions at $\sqrt{s} = 13$ TeV*, J. High Energy Phys. **01**, 173 (2024), doi:10.1007/JHEP01(2024)173 [preprint doi:10.48550/arXiv.2308.01253].

[19] ATLAS collaboration: G. Aad et al., *Measurements of Higgs bosons decaying to bottom quarks from vector boson fusion production with the ATLAS experiment at $\sqrt{s} = 13$ TeV*, Eur. Phys. J. C **81**, 537 (2021), doi:10.1140/epjc/s10052-021-09192-8 [preprint doi:10.48550/arXiv.2011.08280].

[20] CMS collaboration: A. M. Sirunyan et al., *Measurements of production cross sections of the Higgs boson in the four-lepton final state in proton-proton collisions at $\sqrt{s} = 13$ TeV*, Eur. Phys. J. C **81**, 488 (2021), doi:10.1140/epjc/s10052-021-09200-x [preprint doi:10.48550/arXiv.2103.04956].

[21] ATLAS collaboration: G. Aad et al., *Higgs boson production cross-section measurements and their EFT interpretation in the 4ℓ decay channel at $\sqrt{s} = 13$ TeV with the ATLAS detector*, Eur. Phys. J. C **80**, 957 (2020), doi:10.1140/epjc/s10052-020-8227-9 [preprint doi:10.48550/arXiv.2004.03447].

[22] ATLAS collaboration: G. Aad et al., *Interpretations of the ATLAS measurements of Higgs boson production and decay rates and differential cross-sections in pp collisions at $\sqrt{s} = 13$ TeV*, J. High Energy Phys. **11**, 097 (2024), doi:10.1007/JHEP11(2024)097 [preprint doi:10.48550/arXiv.2402.05742].

[23] ATLAS collaboration: G. Aad et al., *Measurement of the total and differential Higgs boson production cross-sections at $\sqrt{s} = 13$ TeV with the ATLAS detector by combining the $H \to ZZ^* \to 4\ell$ and $H \to \gamma\gamma$ decay channels*, J. High Energy Phys. **05**, 028 (2023), doi:10.1007/JHEP05(2023)028 [preprint doi:10.48550/arXiv.2207.08615].

[24] A. M. Sirunyan et al., *Measurement and interpretation of differential cross sections for Higgs boson production at $\sqrt{s} = 13$ TeV*, Phys. Lett. B **792**, 369 (2019), doi:10.1016/j.physletb.2019.03.059 [preprint doi:10.48550/arXiv.1812.06504].

[25] ATLAS collaboration: G. Aad et al., *Measurements of the Higgs boson inclusive and differential fiducial cross-sections in the diphoton decay channel with pp collisions at $\sqrt{s} = 13$ TeV with the ATLAS detector*, J. High Energy Phys. **08**, 027 (2022), doi:10.1007/JHEP08(2022)027 [preprint doi:10.48550/arXiv.2202.00487].

[26] CMS collaboration: A. Tumasyan et al., *Measurement of the Higgs boson inclusive and differential fiducial production cross sections in the diphoton decay channel with pp collisions at $\sqrt{s} = 13$ TeV*, J. High Energy Phys. **07**, 091 (2023), doi:10.1007/JHEP07(2023)091 [preprint doi:10.48550/arXiv.2208.12279].

[27] ATLAS collaboration: G. Aad et al., *Measurements of the Higgs boson inclusive and differential fiducial cross sections in the 4ℓ decay channel at $\sqrt{s} = 13$ TeV*, Eur. Phys. J. C **80**, 942 (2020), doi:10.1140/epjc/s10052-020-8223-0 [preprint doi:10.48550/arXiv.2004.03969].

[28] CMS collaboration: A. Hayrapetyan et al., *Measurements of inclusive and differential cross sections for the Higgs boson production and decay to four-leptons in proton-proton collisions at $\sqrt{s} = 13$ TeV*, J. High Energy Phys. **08**, 040 (2023), doi:10.1007/JHEP08(2023)040 [preprint doi:10.48550/arXiv.2305.07532].

[29] CMS collaboration: A. M. Sirunyan et al., *Constraints on anomalous Higgs boson couplings to vector bosons and fermions in its production and decay using the four-lepton final state*, Phys. Rev. D **104**, 052004 (2021), doi:10.1103/PhysRevD.104.052004 [preprint doi:10.48550/arXiv.2104.12152].

[30] ATLAS collaboration: G. Aad et al., *Integrated and differential fiducial cross-section measurements for the vector boson fusion production of the Higgs boson in the $H \to WW^* \to e\nu\mu\nu$ decay channel at 13 TeV with the ATLAS detector*, Phys. Rev. D **108**, 072003 (2023), doi:10.1103/PhysRevD.108.072003 [preprint doi:10.48550/arXiv.2304.03053].

[31] CMS collaboration: A. M. Sirunyan et al., *Measurement of the inclusive and differential Higgs boson production cross sections in the leptonic WW decay mode at $\sqrt{s} = 13$ TeV*, J. High Energy Phys. **03**, 003 (2021), doi:10.1007/JHEP03(2021)003 [preprint doi:10.48550/arXiv.2007.01984].

[32] CMS collaboration: A. Hayrapetyan et al., *Measurement of boosted Higgs bosons produced via vector boson fusion or gluon fusion in the $H \to b\bar{b}$ decay mode using LHC proton-proton collision data at $\sqrt{s} = 13$ TeV*, J. High Energy Phys. **12**, 035 (2024), doi:10.1007/JHEP12(2024)035 [preprint doi:10.48550/arXiv.2407.08012].

[33] A. Hayrapetyan et al., _Study of WH production through vector boson scattering and extraction of the relative sign of the W and Z couplings to the Higgs boson in proton-proton collisions at $\sqrt{s} = 13$ TeV_, Phys. Lett. B **860**, 139202 (2025), doi:10.1016/j.physletb.2024.139202 [preprint doi:10.48550/arXiv.2405.16566].

[34] A. Hayrapetyan et al., _Measurement of the production cross section of a Higgs boson with large transverse momentum in its decays to a pair of τ leptons in proton-proton collisions at $\sqrt{s} = 13$ TeV_, Phys. Lett. B **857**, 138964 (2024), doi:10.1016/j.physletb.2024.138964 [preprint doi:10.48550/arXiv.2403.20201].

[35] G. Aad et al., _A search for the dimuon decay of the Standard Model Higgs boson with the ATLAS detector_, Phys. Lett. B **812**, 135980 (2021), doi:10.1016/j.physletb.2020.135980 [preprint doi:10.48550/arXiv.2007.07830].

[36] CMS collaboration: A. M. Sirunyan et al., _Evidence for Higgs boson decay to a pair of muons_, J. High Energy Phys. **01**, 148 (2021), doi:10.1007/JHEP01(2021)148 [preprint doi:10.48550/arXiv.2009.04363].

[37] ATLAS collaboration: G. Aad et al., _Search for Higgs boson production in association with a high-energy photon via vector-boson fusion with decay into bottom quark pairs at $\sqrt{s} = 13$ TeV with the ATLAS detector_, J. High Energy Phys. **03**, 268 (2021), doi:10.1007/JHEP03(2021)268 [preprint doi:10.48550/arXiv.2010.13651].

[38] ATLAS collaboration, _Snowmass white paper contribution: Physics with the phase-2 ATLAS and CMS detectors_, Tech. Rep. ATL-PHYS-PUB-2022-018, CERN, Geneva, Switzerland (2022), https://cds.cern.ch/record/2805993.

[39] CMS collaboration, _Sensitivity projections for Higgs boson properties measurements at the HL-LHC_, Tech. Rep. CMS-PAS-FTR-18-011, CERN, Geneva, Switzerland (2018), https://cds.cern.ch/record/2647699.

[40] M. Cepeda et al., _Higgs physics at the HL-LHC and HE-LHC_, CERN Yellow Rep.: Monogr. **7**, 221 (2019), doi:10.23731/CYRM-2019-007.221.

[41] T. Han, G. Valencia and S. Willenbrock, _Structure-function approach to vector-boson scattering in pp collisions_, Phys. Rev. Lett. **69**, 3274 (1992), doi:10.1103/PhysRevLett.69.3274 [preprint doi:10.48550/arXiv.hep-ph/9206246].

[42] T. Figy, D. Zeppenfeld and C. Oleari, _Next-to-leading order jet distributions for Higgs boson production via weak-boson fusion_, Phys. Rev. D **68**, 073005 (2003), doi:10.1103/PhysRevD.68.073005 [preprint doi:10.48550/arXiv.hep-ph/0306109].

[43] E. L. Berger and J. Campbell, _Higgs boson production in weak boson fusion at next-to-leading order_, Phys. Rev. D **70**, 073011 (2004), doi:10.1103/PhysRevD.70.073011 [preprint doi:10.48550/arXiv.hep-ph/0403194].

[44] K. Arnold et al., _Vbfnlo: A parton level Monte Carlo for processes with electroweak bosons_, Comput. Phys. Commun. **180**, 1661 (2009), doi:10.1016/j.cpc.2009.03.006 [preprint doi:10.48550/arXiv.0811.4559].

[45] J. Baglio et al., _VBFNLO: A parton level Monte Carlo for processes with electroweak bosons – Manual for version 3.0_, (arXiv preprint) doi:10.48550/arXiv.1107.4038.

[46] J. Baglio et al., _Release note - VBFNLO 2.7.0_, (arXiv preprint) doi:10.48550/arXiv.1404.3940.

[47] P. Bolzoni, F. Maltoni, S.-O. Moch and M. Zaro, *Higgs boson production via vector-boson fusion at next-to-next-to-leading order in QCD*, Phys. Rev. Lett. **105**, 011801 (2010), doi:10.1103/PhysRevLett.105.011801 [preprint doi:10.48550/arXiv.1003.4451].

[48] P. Bolzoni, F. Maltoni, S.-O. Moch and M. Zaro, *Vector boson fusion at next-to-next-to-leading order in QCD: Standard Model Higgs boson and beyond*, Phys. Rev. D **85**, 035002 (2012), doi:10.1103/PhysRevD.85.035002 [preprint doi:10.48550/arXiv.1109.3717].

[49] F. A. Dreyer and A. Karlberg, *Vector-boson fusion Higgs production at three loops in QCD*, Phys. Rev. Lett. **117**, 072001 (2016), doi:10.1103/PhysRevLett.117.072001 [preprint doi:10.48550/arXiv.1606.00840].

[50] M. Cacciari, F. A. Dreyer, A. Karlberg, G. P. Salam and G. Zanderighi, *Fully differential vector-boson-fusion Higgs production at next-to-next-to-leading order*, Phys. Rev. Lett. **115**, 082002 (2015), doi:10.1103/PhysRevLett.115.082002 [preprint doi:10.48550/arXiv.1506.02660].

[51] J. Cruz-Martinez, T. Gehrmann, E. W. N. Glover and A. Huss, *Second-order QCD effects in Higgs boson production through vector boson fusion*, Phys. Lett. B **781**, 672 (2018), doi:10.1016/j.physletb.2018.04.046 [preprint doi:10.48550/arXiv.1802.02445].

[52] K. Asteriadis, A. Behring, K. Melnikov, I. Novikov and R. Röntsch, *QCD corrections to Higgs boson production and $H \rightarrow b\bar{b}$ decay in weak boson fusion*, Phys. Rev. D **110**, 054017 (2024), doi:10.1103/PhysRevD.110.054017 [preprint doi:10.48550/arXiv.2407.09363].

[53] A. Behring, K. Melnikov, I. Novikov and G. Zanderighi, *Parton-shower and fixed-order QCD effects in Higgs boson production in weak-boson fusion and its decays to bottom quarks*, Phys. Rev. D **112**, 074033 (2025), doi:10.1103/wdgh-1dn3 [preprint 10.48550/arXiv.2507.01448].

[54] T. Liu, K. Melnikov and A. A. Penin, *Nonfactorizable QCD effects in Higgs boson production via vector boson fusion*, Phys. Rev. Lett. **123**, 122002 (2019), doi:10.1103/PhysRevLett.123.122002 [preprint doi:10.48550/arXiv.1906.10899].

[55] F. A. Dreyer, A. Karlberg and L. Tancredi, *On the impact of non-factorisable corrections in VBF single and double Higgs production*, J. High Energy Phys. **10**, 131 (2020), doi:10.1007/JHEP10(2020)131 [preprint doi:10.48550/arXiv.2005.11334].

[56] K. Asteriadis, C. Brønnum-Hansen and K. Melnikov, *Nonfactorizable corrections to Higgs boson production in weak boson fusion*, Phys. Rev. D **109**, 014031 (2024), doi:10.1103/PhysRevD.109.014031 [preprint doi:10.48550/arXiv.2305.08016].

[57] M.-M. Long, K. Melnikov and J. Quarroz, *Non-factorizable virtual corrections to Higgs boson production in weak boson fusion beyond the eikonal approximation*, J. High Energy Phys. **07**, 035 (2023), doi:10.1007/JHEP07(2023)035 [preprint doi:10.48550/arXiv.2305.12937].

[58] C. Brønnum-Hansen, M.-M. Long and K. Melnikov, *Scale dependence of non-factorizable virtual corrections to Higgs boson production in weak boson fusion*, J. High Energy Phys. **11**, 130 (2023), doi:10.1007/JHEP11(2023)130 [preprint doi:10.48550/arXiv.2309.06292].

[59] M. Ciccolini, A. Denner and S. Dittmaier, *Strong and electroweak corrections to the production of a Higgs + 2jets via weak interactions at the Large Hadron Collider*, Phys. Rev. Lett. **99**, 161803 (2007), doi:10.1103/PhysRevLett.99.161803 [preprint doi:10.48550/arXiv.0707.0381].

[60] F. Campanario, T. M. Figy, S. Plätzer and M. Sjödahl, *Electroweak Higgs boson plus three jet production at next-to-leading-order QCD*, Phys. Rev. Lett. **111**, 211802 (2013), doi:10.1103/PhysRevLett.111.211802 [preprint doi:10.48550/arXiv.1308.2932].

[61] F. Campanario, T. M. Figy, S. Plätzer, M. Rauch, P. Schichtel and M. Sjödahl, *Stress testing the vector-boson-fusion approximation in multijet final states*, Phys. Rev. D **98**, 033003 (2018), doi:10.1103/PhysRevD.98.033003 [preprint doi:10.48550/arXiv.1802.09955].

[62] M. Ciccolini, A. Denner and S. Dittmaier, *Electroweak and QCD corrections to Higgs production via vector-boson fusion at the CERN LHC*, Phys. Rev. D **77**, 013002 (2008), doi:10.1103/PhysRevD.77.013002 [preprint doi:10.48550/arXiv.0710.4749].

[63] A. Denner, S. Dittmaier, S. Kallweit and A. Mück, *HAWK 2.0: A Monte Carlo program for Higgs production in vector-boson fusion and Higgs strahlung at hadron colliders*, Comput. Phys. Commun. **195**, 161 (2015), doi:10.1016/j.cpc.2015.04.021 [preprint doi:10.48550/arXiv.1412.5390].

[64] R. Frederix, S. Frixione, V. Hirschi, D. Pagani, H.-S. Shao and M. Zaro, *The automation of next-to-leading order electroweak calculations*, J. High Energy Phys. **11**, 085 (2021), doi:10.1007/JHEP11(2021)085 [preprint doi:10.48550/arXiv.1804.10017].

[65] E. Bothmann et al., *Event generation with Sherpa 3*, J. High Energy Phys. **12**, 156 (2024), doi:10.1007/JHEP12(2024)156.

[66] J. R. Andersen and J. M. Smillie, *QCD and electroweak interference in Higgs production by gauge boson fusion*, Phys. Rev. D **75**, 037301 (2007), doi:10.1103/PhysRevD.75.037301 [preprint doi:10.48550/arXiv.hep-ph/0611281].

[67] J. R. Andersen, J. M. Smillie, T. Binoth and G. Heinrich, *Loop induced interference effects in Higgs boson plus two jet production at the LHC*, J. High Energy Phys. **02**, 057 (2008), doi:10.1088/1126-6708/2008/02/057 [preprint doi:10.48550/arXiv.0709.3513].

[68] A. Bredenstein, K. Hagiwara and B. Jäger, *Mixed QCD-electroweak contributions to Higgs-plus-dijet production at the CERN LHC*, Phys. Rev. D **77**, 073004 (2008), doi:10.1103/PhysRevD.77.073004 [preprint doi:10.48550/arXiv.0801.4231].

[69] R. V. Harlander, J. Vollinga and M. M. Weber, *Gluon-induced weak boson fusion*, Phys. Rev. D **77**, 053010 (2008), doi:10.1103/PhysRevD.77.053010 [preprint doi:10.48550/arXiv.0801.3355].

[70] X. Chen, A. Huss, S. P. Jones, M. Kerner, J.-N. Lang, J. M. Lindert and H. Zhang, *Top-quark mass effects in H+jet and H+2 jets production*, J. High Energy Phys. **03**, 096 (2022), doi:10.1007/JHEP03(2022)096 [preprint doi:10.48550/arXiv.2110.06953].

[71] J. R. Andersen, H. Hassan, A. Maier, J. Paltrinieri, A. Papaefstathiou and J. M. Smillie, *High energy resummed predictions for the production of a Higgs boson with at least one jet*, J. High Energy Phys. **03**, 001 (2023), doi:10.1007/JHEP03(2023)001 [preprint doi:10.48550/arXiv.2210.10671].

[72] M. Bähr et al., *Herwig++ physics and manual*, Eur. Phys. J. C **58**, 639 (2008), doi:10.1140/epjc/s10052-008-0798-9 [preprint doi:10.48550/arXiv.0803.0883].

[73] G. Bewick et al., *Herwig 7.3 release note*, Eur. Phys. J. C **84**, 1053 (2024), doi:10.1140/epjc/s10052-024-13211-9 [preprint doi:10.48550/arXiv.2312.05175].

[74] T. Sjöstrand, S. Mrenna and P. Skands, *PYTHIA 6.4 physics and manual*, J. High Energy Phys. **05**, 026 (2006), doi:10.1088/1126-6708/2006/05/026 [preprint doi:10.48550/arXiv.hep-ph/0603175].

[75] C. Bierlich et al., *A comprehensive guide to the physics and usage of PYTHIA 8.3*, SciPost Phys. Codebases 8 (2022), doi:10.21468/SciPostPhysCodeb.8 [preprint doi:10.48550/arXiv.2203.11601].

C. Bierlich et al., *Codebase release 8.3 for PYTHIA*, SciPost Phys. Codebases 8-r8.3 (2022), doi:10.21468/SciPostPhysCodeb.8-r8.3.

[76] T. Gleisberg, S. Hoeche, F. Krauss, A. Schaelicke, S. Schumann and J. Winter, *SHERPA 1.α, a proof-of-concept version*, J. High Energy Phys. **02**, 056 (2004), doi:10.1088/1126-6708/2004/02/056 [preprint doi:10.48550/arXiv.hep-ph/0311263].

[77] T. Gleisberg, S. Höche, F. Krauss, M. Schönherr, S. Schumann, F. Siegert and J. Winter, *Event generation with SHERPA 1.1*, J. High Energy Phys. **02**, 007 (2009), doi:10.1088/1126-6708/2009/02/007 [preprint doi:10.48550/arXiv.0811.4622].

[78] E. Bothmann et al., *Event generation with Sherpa 2.2*, SciPost Phys. **7**, 034 (2019), doi:10.21468/SciPostPhys.7.3.034 [preprint doi:10.48550/arXiv.1905.09127].

[79] P. Nason and C. Oleari, *NLO Higgs boson production via vector-boson fusion matched with shower in POWHEG*, J. High Energy Phys. **02**, 037 (2010), doi:10.1007/JHEP02(2010)037 [preprint doi:10.48550/arXiv.0911.5299].

[80] S. Frixione, P. Torrielli and M. Zaro, *Higgs production through vector-boson fusion at the NLO matched with parton showers*, Phys. Lett. B **726**, 273 (2013), doi:10.1016/j.physletb.2013.08.030 [preprint doi:10.48550/arXiv.1304.7927].

[81] A. Ballestrero et al., *Precise predictions for same-sign W-boson scattering at the LHC*, Eur. Phys. J. C **78**, 671 (2018), doi:10.1140/epjc/s10052-018-6136-y [preprint doi:10.48550/arXiv.1803.07943].

[82] T. Chen, T. M. Figy and S. Plätzer, *NLO multijet merging for Higgs production beyond the VBF approximation*, Eur. Phys. J. C **82**, 704 (2022), doi:10.1140/epjc/s10052-022-10671-9 [preprint doi:10.48550/arXiv.2109.03730].

[83] B. Jäger and J. Scheller, *Electroweak corrections and shower effects to Higgs production in association with two jets at the LHC*, J. High Energy Phys. **09**, 191 (2022), doi:10.1007/JHEP09(2022)191 [preprint doi:10.48550/arXiv.2208.00013].

[84] M. van Beekveld and S. Ferrario Ravasio, *Next-to-leading-logarithmic PanScales showers for deep inelastic scattering and vector boson fusion*, J. High Energy Phys. **02**, 001 (2024), doi:10.1007/JHEP02(2024)001 [preprint doi:10.48550/arXiv.2305.08645].

[85] C. Bittrich, P. Kirchgaeßer, A. Papaefstathiou, S. Plätzer and S. Todt, *Soft QCD effects in VBS/VBF topologies*, Eur. Phys. J. C **82**, 783 (2022), doi:10.1140/epjc/s10052-022-10741-y [preprint doi:10.48550/arXiv.2110.01623].

[86] T. Figy, S. Palmer and G. Weiglein, *Higgs production via weak boson fusion in the Standard Model and the MSSM*, J. High Energy Phys. **02**, 105 (2012), doi:10.1007/JHEP02(2012)105 [preprint doi:10.48550/arXiv.1012.4789].

[87] K. Asteriadis, F. Caola, K. Melnikov and R. Röntsch, *NNLO QCD corrections to weak boson fusion Higgs boson production in the $H \to b\bar{b}$ and $H \to WW^* \to 4\ell$ decay channels*, J. High Energy Phys. **02**, 046 (2022), doi:10.1007/JHEP02(2022)046 [preprint doi:10.48550/arXiv.2110.02818].

[88] L. Gates, *On evaluation of nonfactorizable corrections to Higgs boson production via vector boson fusion*, Phys. Lett. B **846**, 138191 (2023), doi:10.1016/j.physletb.2023.138191 [preprint doi:10.48550/arXiv.2305.04407].

[89] N. Greiner, S. Höche, G. Luisoni, M. Schönherr and J.-C. Winter, *Full mass dependence in Higgs boson production in association with jets at the LHC and FCC*, J. High Energy Phys. **01**, 091 (2017), doi:10.1007/JHEP01(2017)091 [preprint doi:10.48550/arXiv.1608.01195].

[90] N. Greiner, S. Höche, G. Luisoni, M. Schönherr, J.-C. Winter and V. Yundin, *Phenomenological analysis of Higgs boson production through gluon fusion in association with jets*, J. High Energy Phys. **01**, 169 (2016), doi:10.1007/JHEP01(2016)169 [preprint doi:10.48550/arXiv.1506.01016].

[91] J. R. Andersen, T. Hapola, A. Maier and J. M. Smillie, *Higgs boson plus dijets: Higher order corrections*, J. High Energy Phys. **09**, 065 (2017), doi:10.1007/JHEP09(2017)065 [preprint doi:10.48550/arXiv.1706.01002].

[92] J. R. Andersen, T. Hapola, M. Heil, A. Maier and J. M. Smillie, *Higgs-boson plus dijets: Higher-order matching for high-energy predictions*, J. High Energy Phys. **08**, 090 (2018), doi:10.1007/JHEP08(2018)090 [preprint doi:10.48550/arXiv.1805.04446].

[93] J. R. Andersen, J. D. Cockburn, M. Heil, A. Maier and J. M. Smillie, *Finite quark-mass effects in Higgs boson production with dijets at large energies*, J. High Energy Phys. **04**, 127 (2019), doi:10.1007/JHEP04(2019)127 [preprint doi:10.48550/arXiv.1812.08072].

[94] K. Becker et al., *Precise predictions for boosted Higgs production*, SciPost Phys. Core **7**, 001 (2024), doi:10.21468/SciPostPhysCore.7.1.001 [preprint doi:10.48550/arXiv.2005.07762].

[95] A. Denner, S. Dittmaier, S. Kallweit and A. Mück, *Electroweak corrections to Higgs-strahlung off W/Z bosons at the Tevatron and the LHC with Hawk*, J. High Energy Phys. **03**, 075 (2012), doi:10.1007/JHEP03(2012)075 [preprint doi:10.48550/arXiv.1112.5142].

[96] F. A. Dreyer and A. Karlberg, *Vector-boson fusion Higgs pair production at N^3LO*, Phys. Rev. D **98**, 114016 (2018), doi:10.1103/PhysRevD.98.114016 [preprint doi:10.48550/arXiv.1811.07906].

[97] F. A. Dreyer and A. Karlberg, *Fully differential vector-boson fusion Higgs pair production at next-to-next-to-leading order*, Phys. Rev. D **99**, 074028 (2019), doi:10.1103/PhysRevD.99.074028 [preprint doi:10.48550/arXiv.1811.07918].

[98] W. L. van Neerven and A. Vogt, *NNLO evolution of deep-inelastic structure functions: The non-singlet case*, Nucl. Phys. B **568**, 263 (2000), doi:10.1016/S0550-3213(99)00668-9 [preprint doi:10.48550/arXiv.hep-ph/9907472].

[99] W. L. van Neerven and A. Vogt, *NNLO evolution of deep-inelastic structure functions: The singlet case*, Nucl. Phys. B **588**, 345 (2000), doi:10.1016/S0550-3213(00)00480-6 [preprint doi:10.48550/arXiv.hep-ph/0006154].

[100] G. P. Salam and J. Rojo, *A higher order perturbative parton evolution toolkit (HOPPET)*, Comput. Phys. Commun. **180**, 120 (2009), doi:10.1016/j.cpc.2008.08.010 [preprint doi:10.48550/arXiv.0804.3755].

[101] S. Alioli, P. Nason, C. Oleari and E. Re, *A general framework for implementing NLO calculations in shower Monte Carlo programs: The POWHEG BOX*, J. High Energy Phys. **06**, 043 (2010), doi:10.1007/JHEP06(2010)043 [preprint doi:10.48550/arXiv.1002.2581].

[102] B. Jäger, F. Schissler and D. Zeppenfeld, *Parton-shower effects on Higgs boson production via vector-boson fusion in association with three jets*, J. High Energy Phys. **07**, 125 (2014), doi:10.1007/JHEP07(2014)125 [preprint doi:10.48550/arXiv.1405.6950].

[103] S. Actis, A. Denner, L. Hofer, A. Scharf and S. Uccirati, *Recursive generation of one-loop amplitudes in the Standard Model*, J. High Energy Phys. **04**, 037 (2013), doi:10.1007/JHEP04(2013)037 [preprint doi:10.48550/arXiv.1211.6316].

[104] S. Actis, A. Denner, L. Hofer, J.-N. Lang, A. Scharf and S. Uccirati, *RECOLA—Recursive computation of one-loop amplitudes*, Comput. Phys. Commun. **214**, 140 (2017), doi:10.1016/j.cpc.2017.01.004 [preprint doi:10.48550/arXiv.1605.01090].

[105] L. Hofer, A. Denner and S. Dittmaier, *COLLIER - A fortran-library for one-loop integrals*, Proc. Sci. **211**, 071 (2014), doi:10.22323/1.211.0071.

[106] A. Denner, S. Dittmaier and L. Hofer, *Collier: A fortran-based complex one-loop library in extended regularizations*, Comput. Phys. Commun. **212**, 220 (2017), doi:10.1016/j.cpc.2016.10.013 [preprint doi:10.48550/arXiv.1604.06792].

[107] S. Catani and M. H. Seymour, *A general algorithm for calculating jet cross sections in NLO QCD*, Nucl. Phys. B **485**, 291 (1997), doi:10.1016/S0550-3213(96)00589-5 [preprint doi:10.48550/arXiv.hep-ph/9605323].

[108] S. Dittmaier, *A general approach to photon radiation off fermions*, Nucl. Phys. B **565**, 69 (2000), doi:10.1016/S0550-3213(99)00563-5 [preprint doi:10.48550/arXiv.hep-ph/9904440].

[109] S. Frixione, Z. Kunszt and A. Signer, *Three-jet cross sections to next-to-leading order*, Nucl. Phys. B **467**, 399 (1996), doi:10.1016/0550-3213(96)00110-1 [preprint doi:10.48550/arXiv.hep-ph/9512328].

[110] A. Denner, M. Pellen and G. Pelliccioli, *NLO QCD corrections to off-shell top-antitop production with semi-leptonic decays at lepton colliders*, Eur. Phys. J. C **83**, 353 (2023), doi:10.1140/epjc/s10052-023-11500-3 [preprint doi:10.48550/arXiv.2302.04188].

[111] F. A. Dreyer, A. Karlberg, J.-N. Lang and M. Pellen, *Precise predictions for double-Higgs production via vector-boson fusion*, Eur. Phys. J. C **80**, 1037 (2020), doi:10.1140/epjc/s10052-020-08610-7 [preprint doi:10.48550/arXiv.2005.13341].

[112] B. Biedermann, A. Denner and M. Pellen, *Large electroweak corrections to vector-boson scattering at the Large Hadron Collider*, Phys. Rev. Lett. **118**, 261801 (2017), doi:10.1103/PhysRevLett.118.261801 [preprint doi:10.48550/arXiv.1611.02951].

[113] B. Biedermann, A. Denner and M. Pellen, *Complete NLO corrections to W^+W^+ scattering and its irreducible background at the LHC*, J. High Energy Phys. **10**, 124 (2017), doi:10.1007/JHEP10(2017)124 [preprint doi:10.48550/arXiv.1708.00268].

[114] A. Denner, S. Dittmaier, P. Maierhöfer, M. Pellen and C. Schwan, *QCD and electroweak corrections to WZ scattering at the LHC*, J. High Energy Phys. **06**, 067 (2019), doi:10.1007/JHEP06(2019)067 [preprint doi:10.48550/arXiv.1904.00882].

[115] A. Denner, R. Franken, M. Pellen and T. Schmidt, *NLO QCD and EW corrections to vector-boson scattering into ZZ at the LHC*, J. High Energy Phys. **11**, 110 (2020), doi:10.1007/JHEP11(2020)110 [preprint doi:10.48550/arXiv.2009.00411].

[116] A. Denner, R. Franken, M. Pellen and T. Schmidt, *Full NLO predictions for vector-boson scattering into Z bosons and its irreducible background at the LHC*, J. High Energy Phys. **10**, 228 (2021), doi:10.1007/JHEP10(2021)228 [preprint doi:10.48550/arXiv.2107.10688].

[117] A. Denner, R. Franken, T. Schmidt and C. Schwan, *NLO QCD and EW corrections to vector-boson scattering into W^+W^- at the LHC*, J. High Energy Phys. **06**, 098 (2022), doi:10.1007/JHEP06(2022)098 [preprint doi:10.48550/arXiv.2202.10844].

[118] J. Bellm et al., *Herwig 7.2 release note*, Eur. Phys. J. C **80**, 452 (2020), doi:10.1140/epjc/s10052-020-8011-x [preprint doi:10.48550/arXiv.1912.06509].

[119] S. Gieseke, P. Stephens and B. Webber, *New formalism for QCD parton showers*, J. High Energy Phys. **12**, 045 (2003), doi:10.1088/1126-6708/2003/12/045 [preprint doi:10.48550/arXiv.hep-ph/0310083].

[120] G. Marchesini and B. R. Webber, *Simulation of QCD jets including soft gluon interference*, Nucl. Phys. B **238**, 1 (1984), doi:10.1016/0550-3213(84)90463-2.

[121] B. R. Webber, *A QCD model for jet fragmentation including soft gluon interference*, Nucl. Phys. B **238**, 492 (1984), doi:10.1016/0550-3213(84)90333-X.

[122] S. Plätzer and S. Gieseke, *Coherent parton showers with local recoils*, J. High Energy Phys. **01**, 024 (2011), doi:10.1007/JHEP01(2011)024 [preprint doi:10.48550/arXiv.0909.5593].

[123] S. Alioli et al., *Update of the Binoth Les Houches Accord for a standard interface between Monte Carlo tools and one-loop programs*, Comput. Phys. Commun. **185**, 560 (2014), doi:10.1016/j.cpc.2013.10.020 [preprint doi:10.48550/arXiv.1308.3462].

[124] S. Plätzer and S. Gieseke, *Dipole showers and automated NLO matching in Herwig++*, Eur. Phys. J. C **72**, 2187 (2012), doi:10.1140/epjc/s10052-012-2187-7 [preprint doi:10.48550/arXiv.1109.6256].

[125] P. Nason, *A new method for combining NLO QCD with shower Monte Carlo algorithms*, J. High Energy Phys. **11**, 040 (2004), doi:10.1088/1126-6708/2004/11/040 [preprint doi:10.48550/arXiv.hep-ph/0409146].

[126] S. Frixione and B. R. Webber, *Matching NLO QCD computations and parton shower simulations*, J. High Energy Phys. **06**, 029 (2002), doi:10.1088/1126-6708/2002/06/029 [preprint doi:10.48550/arXiv.hep-ph/0204244].

[127] S. Jadach, G. Nail, W. Płaczek, S. Sapeta, A. Siódmok and M. Skrzypek, *Monte Carlo simulations of Higgs-boson production at the LHC with the KrkNLO method*, Eur. Phys. J. C **77**, 164 (2017), doi:10.1140/epjc/s10052-017-4733-9 [preprint doi:10.48550/arXiv.1607.06799].

[128] J. Bellm, S. Gieseke and S. Plätzer, *Merging NLO multi-jet calculations with improved unitarization*, Eur. Phys. J. C **78**, 244 (2018), doi:10.1140/epjc/s10052-018-5723-2 [preprint doi:10.48550/arXiv.1705.06700].

[129] J. Baglio et al., *Release note: VBFNLO 3.0*, Eur. Phys. J. C **84**, 1003 (2024), doi:10.1140/epjc/s10052-024-13336-x [preprint doi:10.48550/arXiv.2405.06990].

[130] B. Andersson, G. Gustafson and B. Söderberg, *A general model for jet fragmentation*, Z. Phys. C Part. Fields **20**, 317 (1983), doi:10.1007/BF01407824.

[131] T. Sjöstrand, *Jet fragmentation of multiparton configurations in a string framework*, Nucl. Phys. B **248**, 469 (1984), doi:10.1016/0550-3213(84)90607-2.

[132] T. Sjöstrand and P. Z. Skands, *Transverse-momentum-ordered showers and interleaved multiple interactions*, Eur. Phys. J. C **39**, 129 (2005), doi:10.1140/epjc/s2004-02084-y [preprint doi:10.48550/arXiv.hep-ph/0408302].

[133] B. Cabouat and T. Sjöstrand, *Some dipole shower studies*, Eur. Phys. J. C **78**, 226 (2018), doi:10.1140/epjc/s10052-018-5645-z [preprint doi:10.48550/arXiv.1710.00391].

[134] H. Brooks, C. T. Preuss and P. Skands, *Sector showers for hadron collisions*, J. High Energy Phys. **07**, 032 (2020), doi:10.1007/JHEP07(2020)032 [preprint doi:10.48550/arXiv.2003.00702].

[135] S. Höche and S. Prestel, *The midpoint between dipole and parton showers*, Eur. Phys. J. C **75**, 461 (2015), doi:10.1140/epjc/s10052-015-3684-2 [preprint doi:10.48550/arXiv.1506.05057].

[136] L. Lönnblad and S. Prestel, *Matching tree-level matrix elements with interleaved showers*, J. High Energy Phys. **03**, 019 (2012), doi:10.1007/JHEP03(2012)019 [preprint doi:10.48550/arXiv.1109.4829].

[137] L. Lönnblad and S. Prestel, *Merging multi-leg NLO matrix elements with parton showers*, J. High Energy Phys. **03**, 166 (2013), doi:10.1007/JHEP03(2013)166 [preprint doi:10.48550/arXiv.1211.7278].

[138] R. Corke and T. Sjöstrand, *Improved parton showers at large transverse momenta*, Eur. Phys. J. C **69**, 1 (2010), doi:10.1140/epjc/s10052-010-1409-0 [preprint doi:10.48550/arXiv.1003.2384].

[139] A. Buckley and D. Bakshi Gupta, *Powheg-Pythia matching scheme effects in NLO simulation of dijet events*, (arXiv preprint) doi:10.48550/arXiv.1608.03577.

[140] ATLAS collaboration, *Studies on the improvement of the matching uncertainty definition in top-quark processes simulated with Powheg+Pythia 8*, Tech. Rep. ATL-PHYS-PUB-2023-029, CERN, Geneva, Switzerland (2023), https://cds.cern.ch/record/2872787.

[141] P. Nason and C. Oleari, *Generation cuts and Born suppression in POWHEG*, (arXiv preprint) doi:10.48550/arXiv.1303.3922.

[142] F. Krauss, R. Kuhn and G. Soff, *AMEGIC++ 1.0, a matrix element generator in C++*, J. High Energy Phys. **02**, 044 (2002), doi:10.1088/1126-6708/2002/02/044 [preprint doi:10.48550/arXiv.hep-ph/0109036].

[143] T. Gleisberg and S. Höche, *Comix, a new matrix element generator*, J. High Energy Phys. **12**, 039 (2008), doi:10.1088/1126-6708/2008/12/039 [preprint doi:10.48550/arXiv.0808.3674].

[144] T. Binoth et al., *A proposal for a standard interface between Monte Carlo tools and one-loop programs*, Comput. Phys. Commun. **181**, 1612 (2010), doi:10.1016/j.cpc.2010.05.016 [preprint doi:10.48550/arXiv.1001.1307].

[145] S. Höche, F. Krauss, M. Schönherr and F. Siegert, *A critical appraisal of NLO+PS matching methods*, J. High Energy Phys. **09**, 049 (2012), doi:10.1007/JHEP09(2012)049 [preprint doi:10.48550/arXiv.1111.1220].

[146] L. Lönnblad, *Correcting the colour-dipole cascade model with fixed order matrix elements*, J. High Energy Phys. **05**, 046 (2002), doi:10.1088/1126-6708/2002/05/046 [preprint doi:10.48550/arXiv.hep-ph/0112284].

[147] S. Höche, F. Krauss, M. Schönherr and F. Siegert, *QCD matrix elements + parton showers. The NLO case*, J. High Energy Phys. **04**, 027 (2013), doi:10.1007/JHEP04(2013)027 [preprint doi:10.48550/arXiv.1207.5030].

[148] F. Cascioli, P. Maierhöfer and S. Pozzorini, *Scattering amplitudes with open loops*, Phys. Rev. Lett. **108**, 111601 (2012), doi:10.1103/PhysRevLett.108.111601 [preprint doi:10.48550/arXiv.1111.5206].

[149] F. Buccioni, J.-N. Lang, J. M. Lindert, P. Maierhöfer, S. Pozzorini, H. Zhang and M. F. Zoller, *OpenLoops 2*, Eur. Phys. J. C **79**, 866 (2019), doi:10.1140/epjc/s10052-019-7306-2 [preprint doi:10.48550/arXiv.1907.13071].

[150] S. Schumann and F. Krauss, *A parton shower algorithm based on Catani-Seymour dipole factorisation*, J. High Energy Phys. **03**, 038 (2008), doi:10.1088/1126-6708/2008/03/038 [preprint doi:10.48550/arXiv.0709.1027].

[151] T. Gleisberg and F. Krauss, *Automating dipole subtraction for QCD NLO calculations*, Eur. Phys. J. C **53**, 501 (2007), doi:10.1140/epjc/s10052-007-0495-0 [preprint doi:10.48550/arXiv.0709.2881].

[152] J. Alwall et al., *The automated computation of tree-level and next-to-leading order differential cross sections, and their matching to parton shower simulations*, J. High Energy Phys. **07**, 079 (2014), doi:10.1007/JHEP07(2014)079 [preprint doi:10.48550/arXiv.1405.0301].

[153] S. Frixione, *A general approach to jet cross sections in QCD*, Nucl. Phys. B **507**, 295 (1997), doi:10.1016/S0550-3213(97)00574-9 [preprint doi:10.48550/arXiv.hep-ph/9706545].

[154] R. Frederix, S. Frixione, F. Maltoni and T. Stelzer, *Automation of next-to-leading order computations in QCD: The FKS subtraction*, J. High Energy Phys. **10**, 003 (2009), doi:10.1088/1126-6708/2009/10/003 [preprint doi:10.48550/arXiv.0908.4272].

[155] R. Frederix, S. Frixione, A. S. Papanastasiou, S. Prestel and P. Torrielli, *Off-shell single-top production at NLO matched to parton showers*, J. High Energy Phys. **06**, 027 (2016), doi:10.1007/JHEP06(2016)027 [preprint doi:10.48550/arXiv.1603.01178].

[156] V. Hirschi, R. Frederix, S. Frixione, M. V. Garzelli, F. Maltoni and R. Pittau, *Automation of one-loop QCD computations*, J. High Energy Phys. **05**, 044 (2011), doi:10.1007/JHEP05(2011)044 [preprint doi:10.48550/arXiv.1103.0621].

[157] G. Passarino and M. Veltman, *One-loop corrections for e^+e^- annihilation into $\mu^+\mu^-$ in the Weinberg model*, Nucl. Phys. B **160**, 151 (1979), doi:10.1016/0550-3213(79)90234-7.

[158] A. I. Davydychev, *A simple formula for reducing Feynman diagrams to scalar integrals*, Phys. Lett. B **263**, 107 (1991), doi:10.1016/0370-2693(91)91715-8.

[159] A. Denner and S. Dittmaier, *Reduction schemes for one-loop tensor integrals*, Nucl. Phys. B **734**, 62 (2006), doi:10.1016/j.nuclphysb.2005.11.007 [preprint doi:10.48550/arXiv.hep-ph/0509141].

[160] G. Ossola, C. G. Papadopoulos and R. Pittau, *Reducing full one-loop amplitudes to scalar integrals at the integrand level*, Nucl. Phys. B **763**, 147 (2007), doi:10.1016/j.nuclphysb.2006.11.012 [preprint doi:10.48550/arXiv.hep-ph/0609007].

[161] P. Mastrolia, E. Mirabella and T. Peraro, *Integrand reduction of one-loop scattering amplitudes through Laurent series expansion*, J. High Energy Phys. **11**, 128 (2012), doi:10.1007/JHEP11(2012)128 [preprint doi:10.48550/arXiv.1203.0291].

[162] G. Ossola, C. G. Papadopoulos and R. Pittau, *CutTools: A program implementing the OPP reduction method to compute one-loop amplitudes*, J. High Energy Phys. **03**, 042 (2008), doi:10.1088/1126-6708/2008/03/042 [preprint doi:10.48550/arXiv.0711.3596].

[163] H.-S. Shao, *IREGI user's manual*, unpublished.

[164] T. Peraro, *Ninja: Automated integrand reduction via Laurent expansion for one-loop amplitudes*, Comput. Phys. Commun. **185**, 2771 (2014), doi:10.1016/j.cpc.2014.06.017 [preprint doi:10.48550/arXiv.1403.1229].

[165] V. Hirschi and T. Peraro, *Tensor integrand reduction via Laurent expansion*, J. High Energy Phys. **06**, 060 (2016), doi:10.1007/JHEP06(2016)060 [preprint doi:10.48550/arXiv.1604.01363].

[166] T. Sjöstrand et al., *An introduction to PYTHIA 8.2*, Comput. Phys. Commun. **191**, 159 (2015), doi:10.1016/j.cpc.2015.01.024 [preprint doi:10.48550/arXiv.1410.3012].

[167] S. Frixione, P. Nason and C. Oleari, *Matching NLO QCD computations with parton shower simulations: The POWHEG method*, J. High Energy Phys. **11**, 070 (2007), doi:10.1088/1126-6708/2007/11/070 [preprint doi:10.48550/arXiv.0709.2092].

[168] A. Denner, J.-N. Lang and S. Uccirati, *RECOLA2: Recursive computation of one-loop amplitudes 2*, Comput. Phys. Commun. **224**, 346 (2018), doi:10.1016/j.cpc.2017.11.013 [preprint doi:10.48550/arXiv.1711.07388].

[169] T. Ježo and P. Nason, *On the treatment of resonances in next-to-leading order calculations matched to a parton shower*, J. High Energy Phys. **12**, 001 (2015), doi:10.1007/JHEP12(2015)065 [preprint doi:10.48550/arXiv.1509.09071].

[170] J. R. Andersen and J. M. Smillie, *Factorization of the t-channel pole in quark-gluon scattering*, Phys. Rev. D **81**, 114021 (2010), doi:10.1103/PhysRevD.81.114021 [preprint doi:10.48550/arXiv.0910.5113].

[171] J. R. Andersen and J. M. Smillie, *Constructing all-order corrections to multi-jet rates*, J. High Energy Phys. **01**, 039 (2010), doi:10.1007/JHEP01(2010)039 [preprint doi:10.48550/arXiv.0908.2786].

[172] J. R. Andersen and J. M. Smillie, *Multiple jets at the LHC with high energy jets*, J. High Energy Phys. **06**, 010 (2011), doi:10.1007/JHEP06(2011)010 [preprint doi:10.48550/arXiv.1101.5394].

[173] J. R. Andersen, T. Hapola, M. Heil, A. Maier and J. Smillie, *HEJ 2: High energy resummation for hadron colliders*, Comput. Phys. Commun. **245**, 106832 (2019), doi:10.1016/j.cpc.2019.06.022 [preprint doi:10.48550/arXiv.1902.08430].

[174] J. R. Andersen, B. Ducloué, C. Elrick, H. Hassan, A. Maier, G. Nail, J. Paltrinieri, A. Papaefstathiou and J. M. Smillie, *HEJ 2.2: W boson pairs and Higgs boson plus jet production at high energies*, SciPost Phys. Codebases 21 (2023), doi:10.21468/SciPostPhysCodeb.21 [preprint doi:10.48550/arXiv.2303.15778].

J. R. Andersen, B. Ducloué, C. Elrick, H. Hassan, A. Maier, G. Nail, J. Paltrinieri, A. Papaefstathiou and J. M. Smillie, *Codebase release 2.2 for HEJ*, SciPost Phys. Codebases 21-r2.2 (2023), doi:10.21468/SciPostPhysCodeb.21-r2.2.

[175] W. Kilian, T. Ohl and J. Reuter, *WHIZARD—simulating multi-particle processes at LHC and ILC*, Eur. Phys. J. C **71**, 1742 (2011), doi:10.1140/epjc/s10052-011-1742-y [preprint doi:10.48550/arXiv.0708.4233].

[176] M. Moretti, T. Ohl and J. Reuter, *O'Mega: An optimizing matrix element generator*, (arXiv preprint) doi:10.48550/arXiv.hep-ph/0102195.

[177] T. Cridge, *PDF4LHC21: Update on the benchmarking of the CT, MSHT and NNPDF global PDF fits*, SciPost Phys. Proc. 101 (2022), doi:10.21468/SciPostPhysProc.8.101 [preprint doi:10.48550/arXiv.2108.09099].

[178] R. D. Ball et al., *The PDF4LHC21 combination of global PDF fits for the LHC run III*, J. Phys. G: Nucl. Part. Phys. **49**, 080501 (2022), doi:10.1088/1361-6471/ac7216 [preprint doi:10.48550/arXiv.2203.05506].

[179] A. Buckley, J. Ferrando, S. Lloyd, K. Nordström, B. Page, M. Rüfenacht, M. Schönherr and G. Watt, *LHAPDF6: Parton density access in the LHC precision era*, Eur. Phys. J. C **75**, 132 (2015), doi:10.1140/epjc/s10052-015-3318-8 [preprint doi:10.48550/arXiv.1412.7420].

[180] A. Manohar, P. Nason, G. P. Salam and G. Zanderighi, *How bright is the proton? A precise determination of the photon parton distribution function*, Phys. Rev. Lett. **117**, 242002 (2016), doi:10.1103/PhysRevLett.117.242002 [preprint doi:10.48550/arXiv.1607.04266].

[181] A. Denner, S. Dittmaier, M. Roth and D. Wackeroth, *Electroweak radiative corrections to $e^+e^- \to WW \to 4$ fermions in double-pole approximation — the RacoonWW approach*, Nucl. Phys. B **587**, 67 (2000), doi:10.1016/S0550-3213(00)00511-3 [preprint doi:10.48550/arXiv.hep-ph/0006307].

[182] S. Dittmaier and M. Krämer, *Electroweak radiative corrections to W-boson production at hadron colliders*, Phys. Rev. D **65**, 073007 (2002), doi:10.1103/PhysRevD.65.073007 [preprint doi:10.48550/arXiv.hep-ph/0109062].

[183] J. Bendavid et al., *Les Houches 2017: Physics at TeV colliders Standard Model working group report*, (arXiv preprint) doi:10.48550/arXiv.1803.07977.

[184] N. Berger et al., *Simplified template cross sections - stage 1.1 and 1.2*, Tech. Rep. LHCHWG-INT-2025-001, CERN, Geneva, Switzerland (2025), https://cds.cern.ch/record/2922392.

[185] M. Cacciari, G. P. Salam and G. Soyez, *The anti-k_t jet clustering algorithm*, J. High Energy Phys. **04**, 063 (2008), doi:10.1088/1126-6708/2008/04/063 [preprint doi:10.48550/arXiv.0802.1189].

[186] A. Denner and M. Pellen, *Off-shell production of top-antitop pairs in the lepton+jets channel at NLO QCD*, J. High Energy Phys. **02**, 013 (2018), doi:10.1007/JHEP02(2018)013 [preprint doi:10.48550/arXiv.1711.10359].

[187] J. McGowan, T. Cridge, L. A. Harland-Lang and R. S. Thorne, *Approximate N^3LO parton distribution functions with theoretical uncertainties: MSHT20aN^3LO PDFs*, Eur. Phys. J. C **83**, 185 (2023), doi:10.1140/epjc/s10052-023-11236-0 [preprint doi:10.48550/arXiv.2207.04739].

[188] NNPDF collaboration: R. D. Ball et al., *The path to N^3LO parton distributions*, Eur. Phys. J. C **84**, 659 (2024), doi:10.1140/epjc/s10052-024-12891-7 [preprint doi:10.48550/arXiv.2402.18635].

[189] T. Cridge et al., *Combination of aN^3LO PDFs and implications for Higgs production cross-sections at the LHC*, J. Phys. G: Nucl. Part. Phys. **52**, 065002 (2025), doi:10.1088/1361-6471/adde78 [preprint doi:10.48550/arXiv.2411.05373].

[190] D. Amati, A. Bassetto, M. Ciafaloni, G. Marchesini and G. Veneziano, *A treatment of hard processes sensitive to the infrared structure of QCD*, Nucl. Phys. B **173**, 429 (1980), doi:10.1016/0550-3213(80)90012-7.

[191] J. Kodaira and L. Trentadue, *Summing soft emission in QCD*, Phys. Lett. B **112**, 66 (1982), doi:10.1016/0370-2693(82)90907-8.

[192] C. T. H. Davies and W. J. Stirling, *Non-leading corrections to the Drell-Yan cross section at small transverse momentum*, Nucl. Phys. B **244**, 337 (1984), doi:10.1016/0550-3213(84)90316-X.

[193] C. T. H. Davies, B. R. Webber and W. J. Stirling, *Drell-Yan cross sections at small transverse momentum*, Nucl. Phys. B **256**, 413 (1985), doi:10.1016/0550-3213(85)90402-X.

[194] S. Catani, E. D'Emilio and L. Trentadue, *The gluon form factor to higher orders: Gluon-gluon annihilation at small Q_t*, Phys. Lett. B **211**, 335 (1988), doi:10.1016/0370-2693(88)90912-4.

[195] S. Catani, B. R. Webber and G. Marchesini, *QCD coherent branching and semi-inclusive processes at large χ*, Nucl. Phys. B **349**, 635 (1991), doi:10.1016/0550-3213(91)90390-J.

[196] F. Dulat, S. Höche and S. Prestel, *Leading-color fully differential two-loop soft corrections to QCD dipole showers*, Phys. Rev. D **98**, 074013 (2018), doi:10.1103/PhysRevD.98.074013 [preprint doi:10.48550/arXiv.1805.03757].

[197] A. Banfi, G. Corcella and M. Dasgupta, *Angular ordering and parton showers for non-global QCD observables*, J. High Energy Phys. **03**, 050 (2007), doi:10.1088/1126-6708/2007/03/050 [preprint doi:10.48550/arXiv.hep-ph/0612282].

[198] M. Dasgupta, F. A. Dreyer, K. Hamilton, P. F. Monni and G. P. Salam, *Logarithmic accuracy of parton showers: A fixed-order study*, J. High Energy Phys. **09**, 033 (2018), doi:10.1007/JHEP09(2018)033 [preprint doi:10.48550/arXiv.1805.09327].

[199] S. Mrenna and P. Skands, *Automated parton-shower variations in PYTHIA 8*, Phys. Rev. D **94**, 074005 (2016), doi:10.1103/PhysRevD.94.074005 [preprint doi:10.48550/arXiv.1605.08352].

[200] F. Herren, S. Höche, F. Krauss, D. Reichelt and M. Schönherr, *A new approach to color-coherent parton evolution*, J. High Energy Phys. **10**, 091 (2023), doi:10.1007/JHEP10(2023)091 [preprint doi:10.48550/arXiv.2208.06057].

[201] E. Bothmann, M. Schönherr and S. Schumann, *Reweighting QCD matrix-element and parton-shower calculations*, Eur. Phys. J. C **76**, 590 (2016), doi:10.1140/epjc/s10052-016-4430-0 [preprint doi:10.48550/arXiv.1606.08753].

[202] X. Chen et al., *Theory uncertainties of the irreducible background to VBF Higgs production*, (arXiv preprint) doi:10.48550/arXiv.2509.10368.

[203] J. Andersen et al., *Les Houches 2023: Physics at TeV colliders: Standard Model working group report*, (arXiv preprint) doi:10.48550/arXiv.2406.00708.